Generation of hepatocellular cell line capable of supporting the full replication cycle of Hepatitis B Virus

Yao, Wan-Ling

Table of Contents

Abstract

Hepatitis B virus (HBV) has a replication cycle that cannot be completely reproduced with cultured cell lines. In this study, an engineered cell line capable of supporting the complete HBV life cycle was generated from HepG2 cells that overexpress human NTCP – the HBV entry receptor – and also were defective in RIG-I-like receptor signaling through knockdown of the IPS-1 adaptor molecule. The resultant NtG20.i7 cells were susceptible to HBV and its replication was detectable at 14 days post-infection and persisted for at least 35 days with a gradual increase in the HBc-positive cell population. The cells produced infectious viral particles in the culture supernatant and the addition of preS1 peptide, which blocks HBV entry, impaired the persistence of the infection. Lamivudine addition also achieved this through blockade of viral reverse transcription. Electron microscopy observations confirmed that the persistence of the infection can be maintained by continuous release of infectious HBV virions, thus able to support re-infection in fresh NtG20.i7. This system is useful for expanding our basic understanding of HBV replication cycle and screening of anti HBV chemicals.

Abbreviation

HBV	Hepatitis B virus
RLR	RIG-I like receptor
IPS-1	IFNβ-promoter stimulator 1
NTCP	Sodium taurocholate cotransporting polypeptide
LBST	Liver bile acid transporter
3TC	Lamivudine
cccDNA	Covalently closed circular DNA
rcDNA	Relaxed circular DNA
pgRNA	Pregenomic RNA
HCC	Hepatocellular carcinoma
CHB	Chronic hepatitis B
HBc	Hepatitis B core
HBs	Hepatitis B surface

I. Chapter 1: Introduction

1. Thesis overview

HBV is known as a "stealth" virus that evades host immunity. After its entry into hepatocytes via NTCP interaction, the interplay between HBV and host factors is still not well understood. In addressing the host antiviral factors in innate immune responses to HBV infection, it is necessary to characterize the adaptor IPS-1 as an integral antagonistic component to viral replication. Thus IPS-1 was knocked out in the NtG20.i7 cell line, resulting in defective RIG-I-like receptor signaling. Human NTCP was also overexpressed to enhance viral entry into the cell line, resulting in the line's high susceptibility to HBV infection and capability to remain persistently infected for as long as 35 days. This analysis revealed that upon HBV infection, NtG20.i7 cells maintained infection by continuous release of infectious virions and supported their re-infection in new NtG20.i7, thus completing the HBV life cycle. This is the first system useful for basic understanding of the HBV replication cycle and screening of anti-HBV treatments.

2. *Hepatitis B Virus*

HBV belongs to the family hepadnaviridae and is a small, enveloped double-strand DNA (dsDNA) virus, with high species/tissue-specificity [1]. The mature virus consists of a partially duplex, relaxed circular genome of 3.2 kb with a virion (Dane particle) diameter of 42 nm. So far, eight HBV genotypes (A–H) have been identified with a distinct geographic distribution. In China, Southeast Asia and Japan, genotypes B (subtype adw) and C (subtype adr) are the most common; genotypes A (subtype adw) and D (subtype ayw) are mainly in the US and Europe [2,3]. Differences among the HBV genotypes include severity of infection, the potential of the infection to result in hepatocellular carcinoma (HCC) development, the likelihood of complications, and response to therapy or vaccination [4,5]. Commonly, its genome contains four open reading frames (ORFs), polymerase (pol.), surface (sur.), core (c.) and x. Each ORF has its function: pol. encodes reverse transcriptase, responsible for viral replication; sur. encodes three proteins, L-, M- and S-HBs that form the outer viral envelope; c. has two coding proteins, HBc for capsid formation and HBe for secretion (HBeAg is a main marker of viral replication); x function is still not well understood but acts as

an important effector for viral pathogenesis and oncogenesis [6].

2-1 Clinical and epidemiologic impact of HBV infection

Hepatitis B is a DNA viral infection that affects the liver and can cause cirrhosis, chronic hepatitis B (CHB), hepatocellular carcinoma (HCC), and liver damage worldwide, resulting in 1.2 million deaths annually worldwide [7]. It has been well known that this virus is transmitted via two pathways: one is through contact with the blood or other body fluids of an infected person; another is spread from mother to child at birth, so-called vertical transmission or exposure to infected blood, so-called horizontal transmission [8]. HBV remains a major global health issue with potential for life-threatening liver damage in both acute and chronically infected patients. During initial HBV infection, most of patients have no obvious symptoms but some do present with tiredness, vomiting, yellowish skin, dark urine and abdominal pain [4,9,10]. The infection itself rarely causes death and in fact most patients with chronic disease present no symptoms. However, gradually and eventually, cirrhosis and liver cancer may develop.

2-2 HBV replication cycle

A mature virion, also known as Dane particle, consists of an outer lipid envelope and a capsid enclosing an incomplete plus-strand (+) and complete minus-strand (-) DNA [11]. During the process of viral entry into the cytoplasm, nucleocapsids with uncoating envelope facilitate transport to the nucleus, where the relaxed circular DNA (rcDNA) is repaired by host cellular machinery. The incomplete (+)-DNA strand is completed by the viral polymerase and RNA-primers [12,13]. Thus, the complete dsDNA in the nucleus is converted into covalently closed circular DNA (cccDNA) by covalent ligation. cccDNA serves as the template for all viral RNA species through the cellular transcriptional machinery and is crucial for the persistence of HBV infection. One of the cccDNA transcripts, termed pregenomic RNA (pgRNA), is reverse transcribed into (-)-DNA, which is further converted into the rcDNA. Other viral RNA transcripts act as mRNA for different viral proteins. rcDNA encapsidated by nucleocapsids is either re-entered to the nucleus for maintaining cccDNA levels or enveloped by lipids and HBs, and then released outside of the cell. The released viral particles mainly consist of two types: non-infectious subviral spherical or filamentous particles (SVPs) of 22 nm

diameter, and infectious virions of 42 nm, so-called Dane particles [14].

2-3 Experimental models

In the initial phase of research on HBV have been based primarily on infection studies performed in chimpanzees and with HBV-related hepadnaviruses in their hosts [15]. Studies on duck HBV (DHBV) infection in ducks allowed the elucidation of the details of the viral life cycle. Wood-chuck HBV (WHBV) infections have revealed viral sensing factors against infection. Despite the variety of host species, the chimpanzee is the only immunocompetent host that is fully susceptible to HBV infection [1,4,6,15-17]. *Tupaia belangeri*, the small squirrel-like animal, has also been extensively used for infection studies. However due to the restraints encountered using chimpanzees and other animal models with HBV-related viruses, small and well-characterized *in vivo* and *in vitro* systems still need to be constructed and developed. Driven by the need for a well-defined, inbred, small and low-cost system, most research currently focus on the development of mice systems and cell lines [18-21]. Commonly used systems for understanding the viral activities are transgenic mice or hepatocytes with specific aspects of HBV replication and the oncogenic potential of distinct viral genes.

Notably, a terminally redundant overlength 1.3-fold HBV genome construct was used to generate HBV-replicating transgenic mice, and cell lines such as HepG2.2.15, HepAD38, and ES2 were developed to elucidate the mechanism of host-virus interaction. Although these systems demonstrate the general features of immunity and virus-host interactions, they do not accurately represent the natural HBV infection. An earlier report showed that the relatively short spans of viral replication also made further investigation by hydrodynamic injection in mice difficult [22]. Thus, three systems for natural HBV infection were established to investigate the interplay in immunity: i) chimeric mouse models which have humanized livers; ii) HepaRG, which is a human bipotent progenitor liver cell line and capable of differentiating into biliary-like and hepatocyte-like cells; and iii) primary human hepatocytes (PHH) [20,22,23].

2-4 Current clinical therapies

HBV can survive outside the body for at least 7 day, allowing the virus to infect an unvaccinated person [4]. Once a person is infected the average incubation period of the virus is 75 days (may vary from 30 to 180 days). HBeAg may be detected from 30 to 60 days [7]. A number of blood tests are available to diagnose and monitor the patients. During the initial phase of infection, patients are seropositive for HBeAg, which indicates that viral replication is active and viral particles are present in their blood and body fluids. The presence of HBeAg in hepatitis B patients correlates with high contagion. In CHB, HBsAg in patients is detectable for at least 6 months or more regardless of concurrent HBeAg. The persistence of HBsAg is the major marker of risk for developing chronic liver disease and HCC later in life [10,24,25]. To prevent this public disease, a vaccine against HBV has been available since 1982 and it is 95% effective when administered through prophylaxis. Currently there is no effective antiviral therapy for patients with acute hepatitis B infection. However, patients with CHB could be treated with oral antiviral drugs and interferon injection. These therapies reduce viral replication and improve long-term survival. CHB patients need to

take oral treatments (tenofovir or entecavir) persistently for their lifetime because these drugs can suppress viral replication while failing to eradicate the virus. Alternatively, interferon treatment is able to shorten the antiviral treatment duration [25-28]. Both treatments for CHB possess disadvantages. Use of tenofovir or entecavir, the most potent medication, has some side effects and risk for drug resistance. Interferon treatment may not be widely available due to its high cost and the need to carefully monitor for significant adverse effects. The worst sequelae of CHB are liver cirrhosis and cancer. For these, surgical operation or chemotherapy may prolong lifespan. Liver transplantation is also considered as an option. Despite this, treatment options on hepatitis B are still limited, and the outcome for therapies is generally poor. Presently, vaccination and implementation of blood safety strategies are the most effective ways to prevent transmission of HBV.

3. NTCP, a functional receptor for HBV entry

The human *SLC10A1* (solute carrier family 10 member 1) gene encodes sodium-taurocholate co-transporting polypeptide (NTCP), also is also known as the Na^+/bile acid co-transporter or liver bile acid transporter (LBST), with a mass of 56 kDa [29]. In 2012, NTCP was identified as an HBV entry receptor which, when overexpressed, supports the establishment of a susceptible cell line for HBV infection. This finding allowed a deeper investigation for understanding HBV infection and it provided a door to explore new therapies [30,31].

3-1 Fundamental functions

NTCP locates at the basolateral membrane of hepatocytes, where it functions in the hepatic influx of conjugated bile salts from portal blood circulation [29]. Mainly, it binds to a complex containing two Na^+ ions and bile acid for uptake, but like other transporters, is also able to bind to other molecules, like steroid hormones, thyroid hormones, drug-conjugated bile salts and a variety of xenobiotics. Many reports have shown that various NTCP single nucleotide polymorphisms (SNPs) alter its transporter activity, but none have mentioned that such defects cause any serious disease [32]. These polymorphism in NTCP

variants have been found to be dependent on ethnicity. For instance: i) the S267F variant is seen with a 7.5% allele frequency in Chinese Americans with deficient bile acid uptake but with estrone sulfate, a non-bile acid substrate; ii) I223T variant with a 5.5% of allele frequency in African Americans, with reduction of transporter activity and of NTCP localization on the plasma membrane; iii) S267F and A64T variants seen respectively with 3.1% and 1% allele frequencies in Koreans, with a reduction of taurocholic acid uptake. That known NTCP deficiencies do not cause severe diseases makes it difficult to describe the physiological roles of NTCP but may be helpful to consider as a target for antiviral drugs against HBV [33].

3-2 New discovery for interaction with HBV

In 2012, NTCP was identified as a receptor for HBV entry [30]. The HBV surface ORF consists of the region of preS1, preS2 and S, encoding three proteins are the large (LHBs), middle (MHBs) and small (SHBs) surface proteins. LHBs cover the whole surface ORF; MHBs encompass preS2 and S; SHBs comprise S. The preS1 region of HBV surface protein is important for entering the host hepatocytes, following a multiple step process: i) the viral particle attaches to surface

proteoglycans of the host cell with low affinity; ii) associates with functional receptor(s), NTCP or other unknown molecules with a high affinity; iii) gains entry by endocytosis-mediated internalization [31,33-36]. Recently, affinity purification and mass spectrometry analysis of *Tupaia belangeri* NTCP (tsNTCP) determined NTCP, as the host factor with a high affinity to viral entry, can be blocked by preS1-derived lipopeptide. This lipopeptide was also shown to determine the specificity for human NTCP (hNTCP) [37]. Thus, knockdown of NTCP expression by siRNA in PHH or HepaRG resulted in the reduction of HBV infection, while overexpression of NTCP in HepG2 cells conferred susceptibility to HBV infection [38-40]. Further studies showed that certain NTCP mutations, variants like N262A, Q293A/L294A, abrogate the binding to preS1 peptide and directly affect HBV infection. The amino acid sequences in NTCP related to HBV infection reside within amino acids 157-165 [37]. Moreover, aa residues 84–87 were proven to be a dominant sequence for NTCP function as a viral entry receptor. This interaction between NTCP and HBV helps clarify the mechanism of viral early infection and may lead to a new target for antiviral drugs.

4. Innate immunity and antiviral responses

Innate immunity is the first line of defense against pathogen invasion [41,42]. This response is not specific to a particular pathogen. Pathogen-associated molecular patterns (PAMPs) are recognized by host sensors, which subsequently activate immune response to eradicate the invading pathogen. It is quite well known that nucleic acid sensing of viruses with different adaptors is indispensable to the initiation of antiviral responses. This critical response, globally called innate immunity, protects hosts from pathogen invasion during the initial time of exposure.

4-1 RLR signaling pathway

The RIG-I-like receptors (RLRs) are a family of cytosolic pattern recognition receptors. This family is composed of retinoic acid-inducible gene (RIG-I), melanoma differentiation-associated gene 5 (MDA5), and laboratory of genetics and physiology 2 (LGP2) [42,43]. RLRs are necessary for detection of viral RNA and initiation of signal transduction, which results in the IRF3/7-dependent expression of interferons (IFNs) and NF-κB-dependent expression of pro-inflammatory cytokines. They share similar structures that all have a DexD/H

box RNA helicase domain and a C-terminal domain (CTD). Only RIG-I and MDA5 both have two N-terminal caspase recruitment domains (CARDs). The DexD/H box RNA helicase domain has ATPase activity. CTD participates to RNA binding along with the helicase domain while CARD mediates downstream signaling by interacting with the CARD of Interferon-beta promoter stimulator 1 (IPS-1) [44]. Notably, LGP2 is unable to interact with IPS-1, therefore it cannot signal. It is, however, considered as a positive or negative regulator for RIG-I and MDA5 [45,46]. Basically, RIG-I and MDA5 trigger similar signaling pathways but recognize different signatures. RIG-I preferentially recognize the following signatures: i) short 5' triphosphorylated double-stranded RNA (5'ppp dsRNA); ii) short 5'ppp ssRNA containing double-stranded regions; iii) relatively short (<1000 bp) dsRNA lacking a 5' phosphate or containing a 5' monophosphate. On the other hand, MDA5 senses long dsRNA (>1000 bp) molecules. Viral RNA binds to RIG-I/MDA5; this triggers conformational change of the sensors from their inactive to active form. As a result, the CARDs of RIG-I/MDA5 are exposed to interact with the CARD of IPS-1 on the mitochondrial membrane. This allows activation of downstream signaling pathway. Dimerization of IPS-1 leads to its

interaction with multiple adaptor proteins, like TRAF-2/6 and TRADD, which recruit TRAF-3 and TANK to activate TBK1 and IKKε. TBK1 and IKKε, in turn, phosphorylate IRF3/7, which then translocate from cytosol to nucleus. This cascade of event culminates into the production of type I/III IFNs. On the other hand, the IPS-1-TRADD complex induces phosphorylation of IκB, which promotes the NF-κB production.

4-2 The interplay between HBV and immunity

HBV is a stealth virus that actively avoids recognition by host innate immunity. Upon HBV infection, RIG-I and MDA5 potentially recognize viral RNAs. Previous reports have shown that viral evasion is caused by inhibition effects of viral proteins on host factors [47-50]. In human hepatocellular cell lines, HBV polymerase impairs innate immune responses by blocking IRF activation. The regulatory viral protein HBx binds to IPS-1 and promote its degradation through ubiquitination. As a result the RIG-I-dependent IFN-β production is inhibited [22]. The TLRs signaling pathway, well known for promoting dendritic cell maturation, is also attenuated by HBV infection [23,51,52]. HBV Dane particles and HBsAg together with HBeAg has been reported to abrogate the TLR signaling pathway

via the suppression of IFNs and ISGs expression. In HBV transgenic mice, HBV replication was controlled by TLR activation. Other components, like DCs, NKs, and NKT cells are targeted by HBV and activated during acute hepatitis [52,53].

II. Chapter 2:

Cytoplasmic RNA sensing mechanism negatively regulates HBV expression

1. Results

1-1 IPS-1 inhibits HBV replication

ES2, the modified 1.3-fold HBV genome in HepG2 was selected by hygromycin B. The transfected *BclI*-harboring plasmid is derived from plasmid pHBV1.3, containing a 1.3-fold HBV genome, which belongs to subtype ayw, in a modified pUC13 vector backbone. The viral transcription of pgRNA is controlled by its own core promoter and enhancer I and II regulatory elements [55]. This cell line has a chromosomally integrated HBV DNA copy and constitutively produces HBV antigens and infectious HBV with a single *BclI* site at the 5' end, thus making it useful for examining various antiviral molecules on HBV replication. Key components of antiviral innate immune responses by were first knocked down with siRNA. IPS-1 is a crucial adaptor for RLR signaling and its deficiency abrogates RLR-mediated antiviral signaling [44] and STING is an important molecule in the cytoplasmic DNA-sensing pathway [53]. In figure 1A, siRNA

targeted to IPS-1 and STING significantly lessened respective protein expressions. Intracellular HBc was detectable and its level was markedly augmented by IPS-1 knockdown in ES2 cells; however, knockdown of STING did not interfere its expression. As described before, formation of cccDNA in ES2 cells has been reported by digestion of HBV cDNA with *Bcl*I and *Ssp*I, where 132 and 200 bp fragments signify that the cDNA is derived from cccDNA (Fig. 1B). ES2 cells subjected to control siRNA exhibited an RT-PCR product of 935 bp; however, intensity of cccDNA detection was low. ES2 cells with a knockdown of IPS-1 expression revealed a dramatic induction in the 935 bp band, as well as bands at 132 and 200 bp, showing that down-regulation of IPS-1 markedly enhanced HBV transcription derived both from the chromosomal integrated HBV and newly formed cccDNA. STING knockdown alone failed to enhance HBV transcription; however, in combination with IPS-1 knockdown resulted in enhanced HBV replication and transcription, as evidenced by mRNA levels for HBc and HBs by RT-PCR (Fig. 1C), as well as HBV DNA release into culture supernatant (Fig. 1D). This finding suggested that IPS-1 negatively regulates HBV replication and release of viral DNA into culture supernatant.

2. *Discussion*

According to the results collected above, down-regulated IPS-1 enhances HBV activity, confirming the crucial antiviral role IPS-1 plays in inhibiting HBV. Due to the ES2's nature as an HBV stably expressing cell line, it is difficult to understand the mechanism of natural HBV evasion of innate immune responses. Thus this prompted further investigation in maintaining HBV infection naturally in other hepatic cell lines through knockdown of IPS-1. Generation of these cell lines would be indispensable in understanding HBV natural infection in vitro.

III. Chapter 3:

Establishment of a human hepatocellular cell line capable of maintaining long-term replication of HBV

1. Results

1-1 Generation of HepG2-derived cell lines, NtG20 and NtG20.i7

To facilitate HBV infection in cell culture, HepG2 cells stably expressing human NTCP, which acts as a receptor for HBV entry [30], was generated by using a construct fusion with turboGFP (tGFP). One of the sorting clones, termed NtG20, showed high level of hNTCP-tGFP expression (Fig. 2A), as well as high susceptibility to HBV infection (Fig. 2D). According to the above results, using NtG20 as the parental cells, an shRNA expression vector for IPS-1 was introduced. The resultant clones were assessed for IPS-1 expression and susceptibility to HBV infection (Fig. 2D). One of the clones, named NtG20.i7, exhibited diminished IPS-1 expression (Fig. 2B) as well as the highest susceptibility to HBV replication (Fig. 2D), and was, therefore, further investigated for this study. Microscopy analysis of these cells confirmed that hNTCP-tGFP was primarily detectable on the plasma membranes of NtG20 and

NtG20.i7, consistent with the localization of NTCP (Fig. 2C). Moreover, expression of hNTCP-tGFP was confirmed and clearly detected by western blot (Fig. 2B). Here, two major cell lines derived from HepG2, as primary materials to study HBV infection *in vitro*.

1-2 Establishment of HBV infection *in vitro*

HBV infectivity in HepG2 and its derivative cell lines was investigated (Fig. 2D). In detail, Hep38.7-Tof (Hep38.7-Tet [54], with additional tetracycline removed) culture supernatant as a HBV source was used (Fig. 3A), since it contained a higher HBV DNA content compared to ES2 cells or HBV-infected sera from human liver chimeric mice (Fig. 3B). A condensed-filter-kit (Materials and Methods) was used to condense the virus by 20-fold. Thus, for each HBV infection experiment the cells were routinely exposed to HBV at 1000 GEq/cell.

1-3 Comparison of HepG2 and its derived cell lines against HBV

To analyze HBV infection and replication in HepG2-derived cell lines, Hep38.7-Tof cell culture supernatant as an HBV inoculum (hereafter named as HBV_{tof}) was used. The prepared cells were exposed to HBV_{tof} at 1,000 GEq/cell and cultivated thereafter as described in Figure 4A. At 21 days post infection without any cell passages, cells were fixed and stained for HBc then analyzed by flow cytometry (Fig. 4B, left panel). Hep38.7-Tof cells expressing HBV showed high expression of HBc as a positive control. The fluorescence profiles of HepG2 cells, with or without HBV infection, were identical, representing that this cell line was hardly infected by HBV_{tof}. However, HBV_{tof}-infected NtG20 cells revealed a minor rise in HBc expression, with NtG20.i7 showing greater HBc expression. Intracellular HBc was quantified to show the amount of HBc-positive cells in these infected cells (Fig. 4B, right panel). Also, after the same treatment at 14 days post-infection, HBc expression was clearly detected in NtG20.i7 cells, not in NtG20 and HepG2, via western blot (Fig. 4C). Taken together, this data suggested that NtG20.i7 cell line has a higher susceptibility to HBV infection with decreased IPS-1 expression.

1-4 HBV infection in PXB and NtG20.i7 cells

The results in Figure 4 prompted me to compare HBV infectivity in NtG20.i7 cells and primary human hepatocytes (PHH). HBV infectivity in PXB cells, which are fresh human hepatocytes isolated from a humanized liver from a chimeric mice, and which are regularly used for HBV infection *in vitro* [55] were also examined. PXB cells stayed HBV replication when exposed to sera from HBV-infected chimeric mice bearing human hepatocytes (HBV_{sera}) (Fig. 5A&5B). NtG20.i7 and PXB cells were infected with HBV_{tof} at 1,000 GEq/cell and cultivated as described in Figure 5A. RT-PCR analysis revealed comparable viral replication between NtG20.i7 and PXB cells at different time points (Fig. 5B). It showed that viral production, measured as expression of HBc, in both cell lines was induced in a time-dose dependent manner after infection. HBV_{sera}-infected PXB cells were included as a positive control. To investigate the differences between HBV_{tof}- NTG20.i7 and -PXB cells, they were harvested at 21 days post-infection and viral translation was evaluated by detection of HBc (Fig. 5C). In conclusion, NtG20.i7 cells exhibited comparable viral infectivity and expression compared to PXB cells.

1-5 NtG20.i7 allows long-term maintenance of HBV replication

Although NtG20.i7 cells exhibited susceptibility to HBV, their efficiency was only just above the detection level after 21 days. Therefore, I investigated the effects of longer cultivation after exposure to HBV at 1,000 GEq/cell. NtG20.i7 cells were infected for up to 35 days without a single cell passage, as described in Fig. 6A. HBc protein expression was determined by western blot (Fig. 6B) and was evidently detectable at 21 dpi, and continued to increase up to 35 dpi. Cellular mRNA levels for HBc, HBs, and NTCP, and HBV DNA relative levels in culture supernatant, were raised at 14 to 35 dpi (Fig. 6C, D). These results indicated that the viral replication was time-sensitive. Finally, flow cytometry analysis indicated that HBc expression significantly increased from 14 dpi to 21 dpi, and continued to increase up to 35 dpi (Fig. 6E). Taken together, these findings showed that NtG20.i7 cells were able to sustain a long-term persistent viral infection and replication.

1-6 HBV process of *de novo* replication in NtG20.i7

The above results showed that NtG20.i7 cells were susceptible to HBV and maintained its replication for 35 days. The observed long-term continuation of HBV expression may be due to two mechanisms: i) steady propagation of initially infected cells, and ii) *de novo* infection through newly produced viral Dane particles. To investigate these possibilities, the LHBs peptide, myr-47WT, which interferes with entry of HBV into host cells was utilized [30,38,56,57]. NtG20.i7 cells were infected with HBV, as described in Fig. 7A, at 1,000 GEq/cell, further treated with myr-47WT or a mutant myr-47N9K, which lacks inhibitory activity at 21 days. For comparison, infected cells were also treated with Lamivudine (3TC), a reverse transcriptase inhibitor [26]. Harvest of culture supernatants were qualified by HBs ELISA (Fig. 7B), and cells were examined by a microplate immunostaining assay for HBc (Fig. 7C, Materials and Methods). These findings indicated that expression of HBs and HBc was blocked by the myr-47WT peptide, but not by the mutant, implying *de novo* infection by newly formed infectious viral particles. To address the effect of these treatments on HBV_{tof}-infected NtG20.i7 cells, FACS analysis to examine HBc expression

levels was performed (Fig. 7D). 3TC and Myr-47WT treated cells showed a reduction in HBc expression compared to the control. The HBV DNA expression level was also quantified and a similar tendency to the HBc expression level was observed (Fig. 7E). Therefore, HBV expression was 3TC sensitive, suggesting that a canonical HBV life cycle occurs in these infected cells. 3TC blocks viral reverse transcriptase activities, thus interrupting new cccDNA formation. After 3TC treatment, though some residual cccDNA allowed transcription of pgRNA and mRNAs, producing HBs, HBc and HBx, it still widely inhibited viral activities. Therefore, in our infection assay, 3TC and preS1 peptide proved to be efficient inhibitors of HBV.

1-7 Examination of re-infection

To further address the release of infectious HBV (virions), the culture supernatant from infected NtG20.i7 for HBV infectivity was examined. The culture supernatant of HBV_{tof}-infected NtG20.i7 cells was harvested at 21 dpi, concentrated (indicated as HBV_{inf}), and introduced to naive NtG20.i7 cells, as described in Fig. 8A. The HBV_{inf} -infected cells were analyzed for HBc by immunoblotting (Fig. 8B), and cellular RNAs was examined for HBc, HBs, and NTCP by RT-PCR (Fig. 8C, D, E). Although this data was generated from supernatant collected at 14 days post-infection, this time point was still sufficient to show that viral expression was achieved in the HBV_{inf}-infected NtG20.i7 cells. The results demonstrate that HBV_{tof}-infected NtG20.i7 cells produce infectious HBV, which supports causing re-infection in new NtG20.i7 cells (HBV_{inf}-infected NtG20.i7).

1-8 Detection of cccDNA and pgRNA in HBV-infected NtG20.i7 cells

According to the above results, I speculated that NtG20.i7 cells support the full HBV replication cycle. Since cccDNA is a fundamental template for HBV transcription and replication [58], I attempted to detect it. In figure 9A, the Southern blot showed that NtG20.i7 cells infected with HBV for 35 days contained 2 viral DNA species, with size of 3.2 and 2.1 kb. These bands were scrutinized by T5 exonuclease digestion (Fig. 9B) and were recognized as relaxed circular DNA (rcDNA) and cccDNA, respectively. Due to the presence of cccDNA, I explored further for the presence of its transcription products; pgRNA and other mRNAs, via Northern blot (Fig. 9C). Three viral RNA species were detected, at positions 3.5, 2.4/2.1, and 0.7 kb, which corresponded to pgRNA/precore RNA, S RNA, and X RNA. This detection confirmed the result of figure 9A&B, the presence of cccDNA, and further processes of viral transcription and then translation. HBV_{tof}-infected NtG20.i7 cells were cultured for 28 days, and upon harvesting it was discovered that a high proportion of cells were positive for HBc (Fig. 9D): the average ratio was found to be 52.8±6.4%, compared to 88.3±3.2% for Hep38.7-Tof cells, as indicated by analyzing HBc

staining cells / DAPI staining cells. Taken together, this data suggests that NtG20.i7 cells provided an environment for completing HBV reproduction.

1-9 Formation of virion-like structures in HBV-infected NtG20.i7 cells

This prompted me to observe viral particles in the infected NtG20.i7 cells by various types of electron microscopy (EM), including immuno-electron microscopy (immuno-EM). The EM analyses were prepared in collaboration with Dr. Keiko Shindo and Prof. Takeshi Noda. First, the supernatant of HBV_{tof}-infected NtG20.i7 cells was examined (Fig. 10A). To examine particles related to HBV in the infected cells, ultrathin-section immuno-EM with HBc antibody staining was performed (Fig. 10B). Virion-like structures were discovered in the periphery of cells with HBc staining in the center. Due to antibody reactivity, it was likely that the inner core corresponded to the HBV core, which should be enclosed by a membrane-like structure 42 nm in diameter, according to the stated infectious viral particle. The whole configuration is surrounded by membrane structures of around 100 nm in diameter. Alike structures were observed in Hep38.7-Tof cells, but not in mock-infected cells,

proposing that this is relevant to HBV. Therefore, I reasoned that the infectious HBV (42 nm in diameter) buds into the ER lumen and is transported to the cell periphery, and thus is surrounded by the ER and plasma membranes (illustrated in Fig. 10B, shown in the left diagram). Furthermore, the culture supernatant for NtG20.i7 cells infected with HBV_{tof} for 21 days was detected by negative-staining immuno-EM using HBs antibody (Fig. 10C). A 42 nm diameter structure with anti-HBs reactivity was observed (Fig. 10C, upper panel). This is prospective a mature infectious HBV virion. Similar structures were showed in the culture supernatant of Hep38.7-Tof cells, but not in mock-infected cells. HBs-containing subviral particles were detected in culture supernatants by negative-staining immuno-EM (Fig. 10C, bottom panel). Taken together, the findings of these experiments indicated that these viral structures are relevant to HBV replication, thus further confirming the theory that NtG20.i7 cells can support the full replication cycle of HBV.

2. *Discussion*

Host immunity, especially innate immunity, is the first line of defense against pathogen invasion. It is widely known that innate immune responses are not specific to a particular pathogen and in this way, it is opposite to the adaptive immune responses. To initiate the antiviral responses of the innate immune system, nucleic acid sensing of viruses with different adaptors is indispensable to quickly activate the immune response and help destroy invaders. In this study, the relevant sensing adaptors for HBV infection were explored, and the correlation of nascent innate immune responses and NTCP expression during HBV infection was examined. As results, the RNA virus sensing adaptor, IPS-1 was identified as potential critical antiviral molecule against HBV, and its depletion was found to improve viral activity.

Recent reports have revealed several reasons why HBV does not efficiently and effectively replicate *in vitro*. Different to *in vivo* liver tissue, hepatic cell lines poorly mimic the primary hepatocytes due to a lack of necessary factor(s) and the expression of restriction factor(s), responsible for limiting HBV replication. An earlier study discovered that NTCP is a crucial factor for HBV entry. NTCP is

barely expressed in cell lines such as HepG2 and Huh7, overexpression of which could confer HBV susceptibility (NtG20, Fig. 4B); however, viral replication is much less efficient compared to primary human hepatocytes (Fig. 3B), suggesting additional suppressive mechanisms. This study found that inhibition of IPS-1, an important adaptor for RLR signaling, resulted in enhanced HBV replication in ES2 cells (Fig. 1). This result was strongly related to previous reports that a cytoplasmic viral RNA sensor, RLR, is an additional restriction factor playing a role against HBV [22,59-62]. According to these findings, utilizing NtG20 as parental cells to investigate RLR involvement in the HBV infection system stable IPS-1 knockdown cells were generated. A total of six clones generated from shIPS-1 in NtG20 were examined for IPS-1 expression by western blot and for HBV susceptibility by real-time PCR (Fig. 2D). IPS-1 expression levels negatively correlated with HBV replication among all clones; however, clone 8 was an exception, displaying substantial IPS-1 knockdown, but viral replication was roughly equal to parental NtG20 cells, indicating additional restriction factor(s). Clone 7, named as NtG20.i7 exhibited both the highest propagation of HBV and the lowest IPS-1 expression; thus, this clone for further experiments

was used. Of note, in a widely used cell line HepG2-NTCP-C4 (C4) which is reported to be susceptible to HBV infection [54], IPS-1 knockdown of C4 was also performed and a higher infectivity was observed than in the control. This result indicated that enhancement of HBV infectivity by knockdown of IPS-1 is not restricted to the cell line used in this study. Conveniently, considering NTCP expression on the cell membrane and its expression of green fluorescent, NtG20.i7 might be a good tool to understand the interplay between HBV entry and NTCP during the initial phase.

Notably, NtG20.i7 cells were capable of being stably maintained in culture. Moreover, NtG20.i7 cells possessed comparable, or slightly higher, HBV replication than PXB cells (Fig. 5). While primary hepatocytes (PXB cells) have some restrictions as an experimental model, such as limited cell division and effortless detachment from the culture dish at 28 days, NtG20.i7 cells supported HBV replication for up to 35 days (Fig. 6). HBV gene expression (Fig. 6E) illustrated that HBV gene products in infected cells gradually accumulated during the course of the infection. Since a high proportion of cells were infected at 35 days, the cytopathic effects displayed were not considered significant. These

features are consistent with HBV persistence *in vivo*. Consequently, with improved culture conditions, NtG20.i7 has the potential to allow HBV replication for an extended time period.

All results showed that *de novo* infection through HBV Dane particles mediated this long-term infection (Fig. 7&8). In line with this notion, the culture supernatant of HBV-infected NtG20.i7 cells contained HBV particles, including both infectious virion and non-infectious subviral particles which were observed using electron microscopy (Fig. 10C). Moreover, ultra-sectioning of HBV-infected NtG20.i7 cells revealed that enveloped HBV particles are surrounded by multiple membrane structures located on the cell surface. These structures are similar to a previous report that virus particle-containing vesicles (VCVs) were observed in duck HBV-infected cells [12,63]. I speculated that these structures correspond to enveloped HBV budded into the ER lumen and transported to the cell periphery. The mechanism of how these HBV virions surrounded by multiple membranes are released into the culture medium is still not well known. This system, HBV/NtG20.i7, will be useful for elucidation of this mechanism.

In summary, the establishment of a HepG2-derived clone, NtG20.i7 was reported in this study. NtG20.i7 cells supported the HBV replication cycle with comparable efficiency to primary human hepatocytes (PXB cells). Due to its immortal characteristic, NtG20.i7 can allow HBV replication for at least 35 days, during which viral expression gradually continues to be induced. Moreover, HBV-infected NtG20.i7 cells produced infectious HBV and released them into the culture supernatant. This unique cell culture system is useful for understanding the molecular mechanisms of HBV replication through a combination of gene overexpression, knockdown, and knockout techniques. Practically, this system may be applied to large-scale antiviral drug screening *in vitro,* plus the generation of tissue culture-adapted HBV clones, which will further improve HBV replication *in vitro*.

Figures and Legends

Figure 1

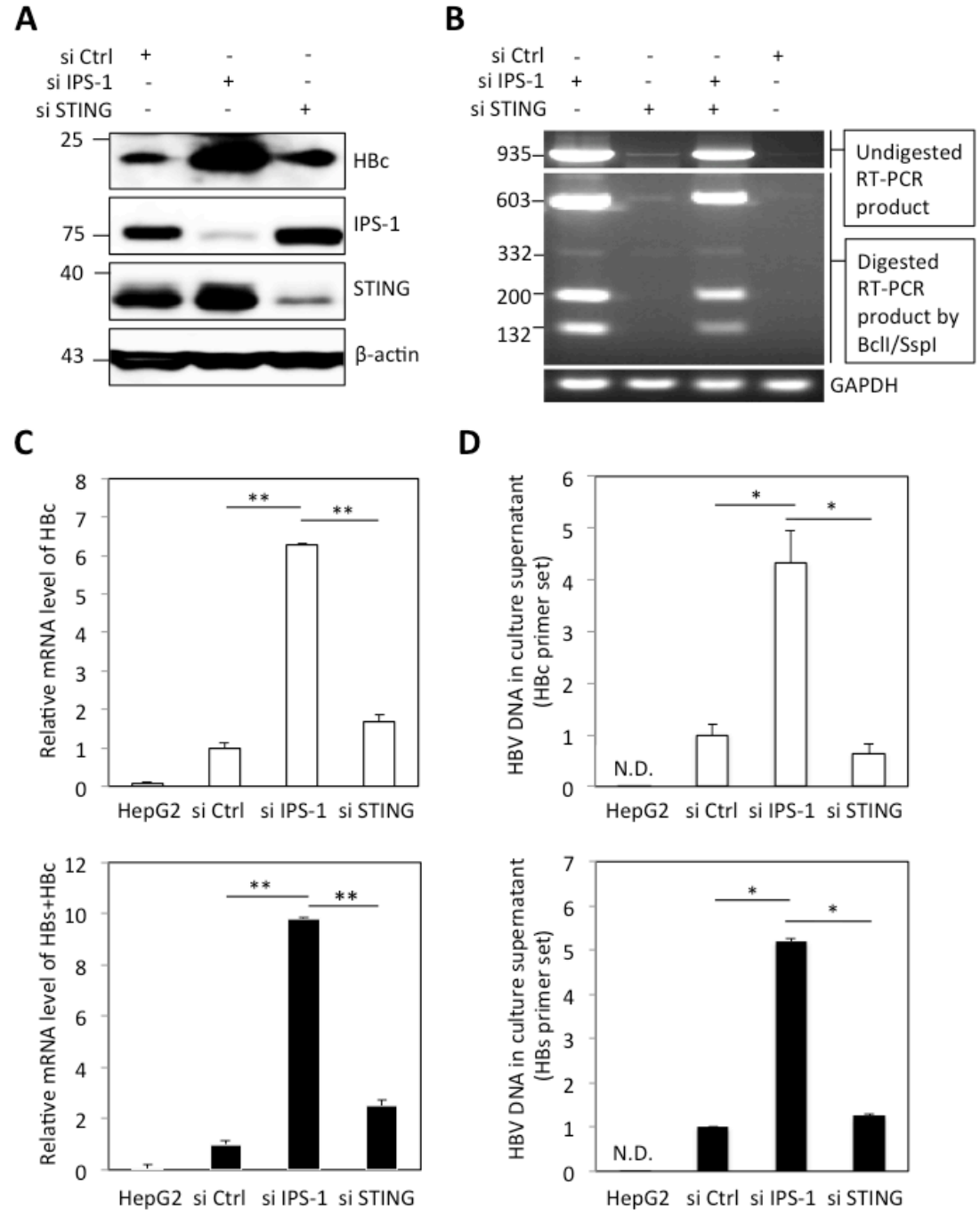

Fig. 1. Knockdown of IPS-1 and STING in ES2 cells

ES2 cells were transfected with control siRNA (siCtrl), siRNA responsed to IPS-1 (siIPS-1), or STING (siSTING) for 5 days. (A) Examination for expression of HBc, IPS-1, and STING by immunoblotting. β-actin served as a loading control. Positions of size markers are shown on the left (kDa). (B) Detection of cccDNA by RT-PCR and restriction enzyme digestion. HBV transcripts of ES2 cells, which had been transfected with the indicated siRNA (+), were subjected to RT-PCR as described in the Materials and Methods, and the products were digested with *Bcl*I and *Ssp*I followed by agarose gel electrophoresis. Fragment sizes, as determined by size markers, are shown on the left (bp). The 200 and 132 bp fragments indicate the transcript of the cccDNA. (C) Induction of HBc and HBs by IPS-1 knockdown. Examination for expression of HBc and HBs mRNA by real-time PCR. The relative mRNA levels are indicated by considering the level of expression in control siRNA-transfected cells to be 1. (D) Up-regulation of HBV DNA release in the culture medium by IPS-1 knockdown. The culture supernatants of cells in (C) were collected and subjected to DNA extraction by smi-TEST (Materials and Methods). The DNA was quantified by qPCR using specific primer sets for HBc and HBs, respectively. The relative DNA levels are indicated by considering the level of expression in control siRNA-transfected cells to be 1.

* $p < 0.05$, ** $p < 0.01$

Figure 2

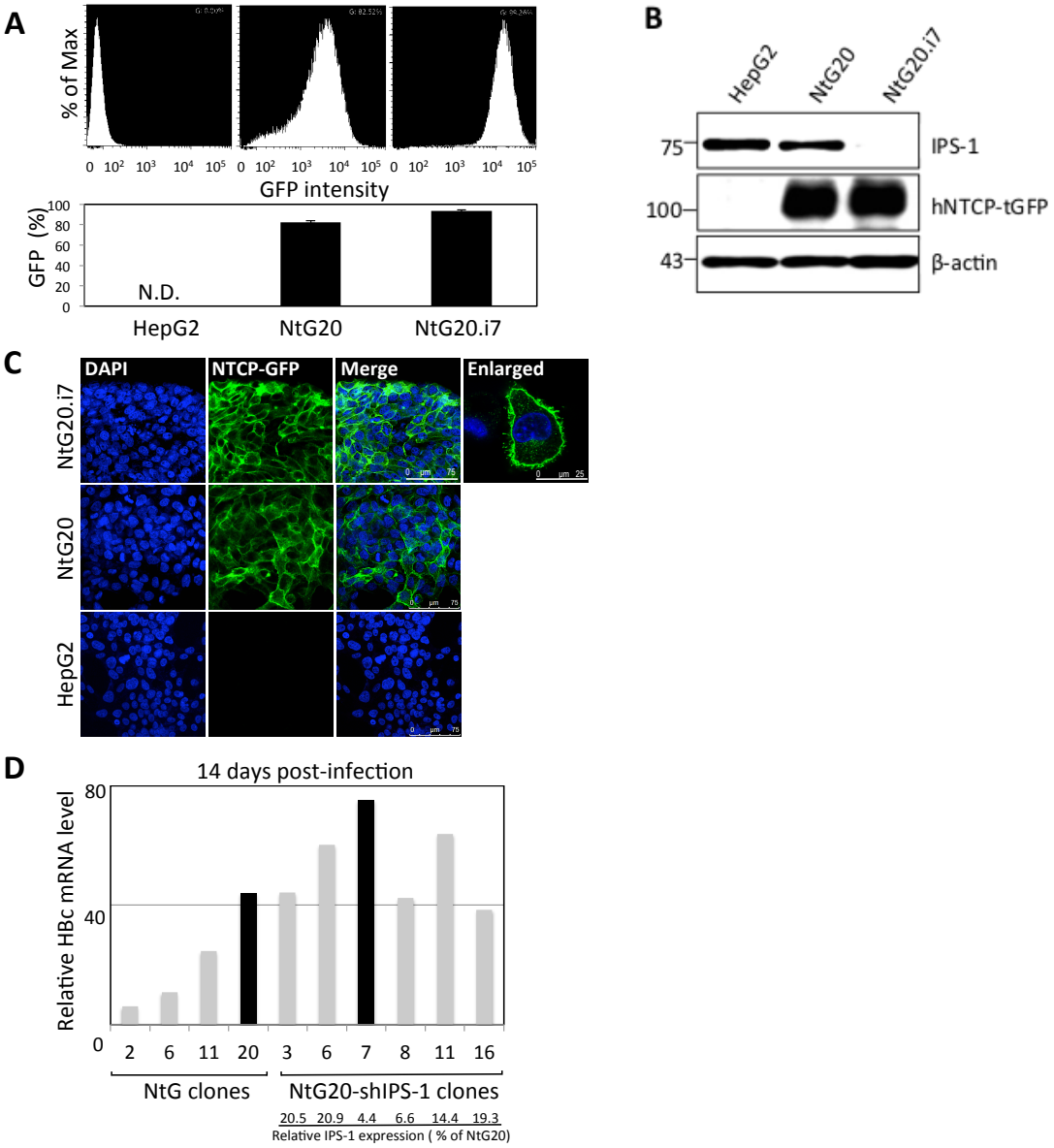
A
% of Max
GFP intensity
GFP (%)
N.D.
HepG2
NtG20
NtG20.i7
B
HepG2
NtG20
NtG20.i7
75
100
43
IPS-1
hNTCP-tGFP
β-actin
C
DAPI
NTCP-GFP
Merge
Enlarged
NtG20.i7
NtG20
HepG2
D
14 days post-infection
Relative HBc mRNA level
80
40
0
2 6 11 20 3 6 7 8 11 16
NtG clones
NtG20-shIPS-1 clones
20.5 20.9 4.4 6.6 14.4 19.3
Relative IPS-1 expression (% of NtG20)

Fig. 2. Generation of NtG20 and NtG20.i7 cell lines

HepG2 cells were transfected with an expression vector encoding the human NTCP-turbo GFP fusion protein (hNTCP-tGFP, Materials and Methods). After drug selection and FACS sorting for GFP, a clone (NtG20) expressing a high level of hNTCP-tGFP was obtained. NtG20 cells were transfected with an expression vector encoding for shRNA for IPS-1 (shIPS-1). The transfectants were colony purified and screened for low expression of IPS-1. NtG20.i7, with efficient down-regulation of IPS-1 was selected. (A) Expression of hNTCP-tGFP in HepG2, NtG20, and NtG.i7 cells was analyzed by FACS (top), and the GFP-positive cell population was quantified (bottom). (B) Expression of IPS-1, hNTCP-tGFP, and β-actin were examined by immunoblotting using respective antibodies. Fragment sizes, as determined by size markers, are shown on the left (kDa). (C) Expression of hNTCP-tGFP was localized to the cell surface. Expression of tGFP (green) was investigated by confocal microscopy. Nuclei were stained using DAPI (blue). (D) HBV infection in HepG2-derived cell lines. NtG clones and NtG20-shIPS-1 clones were infected with HBV at 1000 GEq/cell. At 14 dpi, the intracellular mRNA of HBc was analyzed by real-time PCR. For NtG20 and NtG20.i7 clones, IPS-1 expression was determined and quantified by Western blotting. Relative IPS-1 expression levels were indicated.

Figure 3

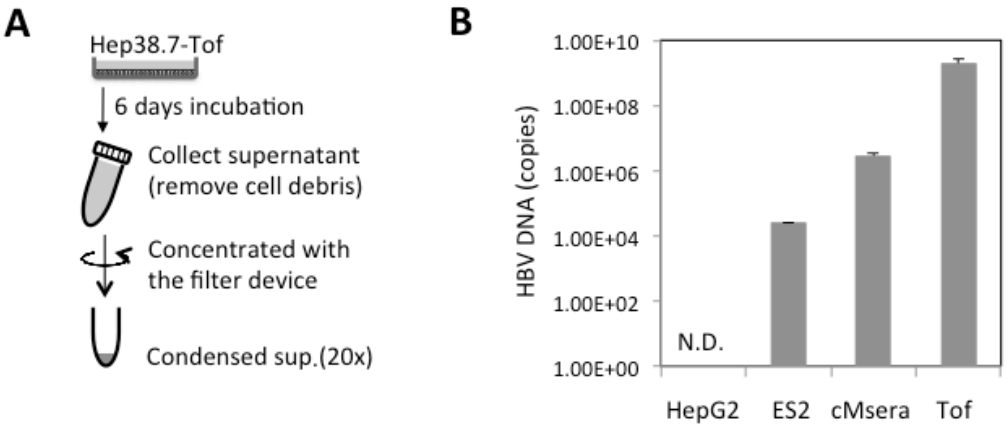
A
Hep38.7-Tof
6 days incubation
Collect supernatant
(remove cell debris)
Concentrated with
the filter device
Condensed sup.(20x)
B
HBV DNA (copies)
1.00E+10
1.00E+08
1.00E+06
1.00E+04
1.00E+02
1.00E+00
N.D.
HepG2
ES2
cMsera
Tof

Fig. 3. Establishment of HBV infection

(A) Preparation of HBV inoculum. Six-day culture media of Hep38.7-Tet (in the absence of tetracycline) cells were harvested and condensed by 20-fold, as described in the Materials and Methods. (B) HBV DNA content of the condensed culture supernatant was examined for HBV DNA by real-time PCR. Chimeric mouse serum (cMserum) was similarly quantified for comparison.

Figure 4

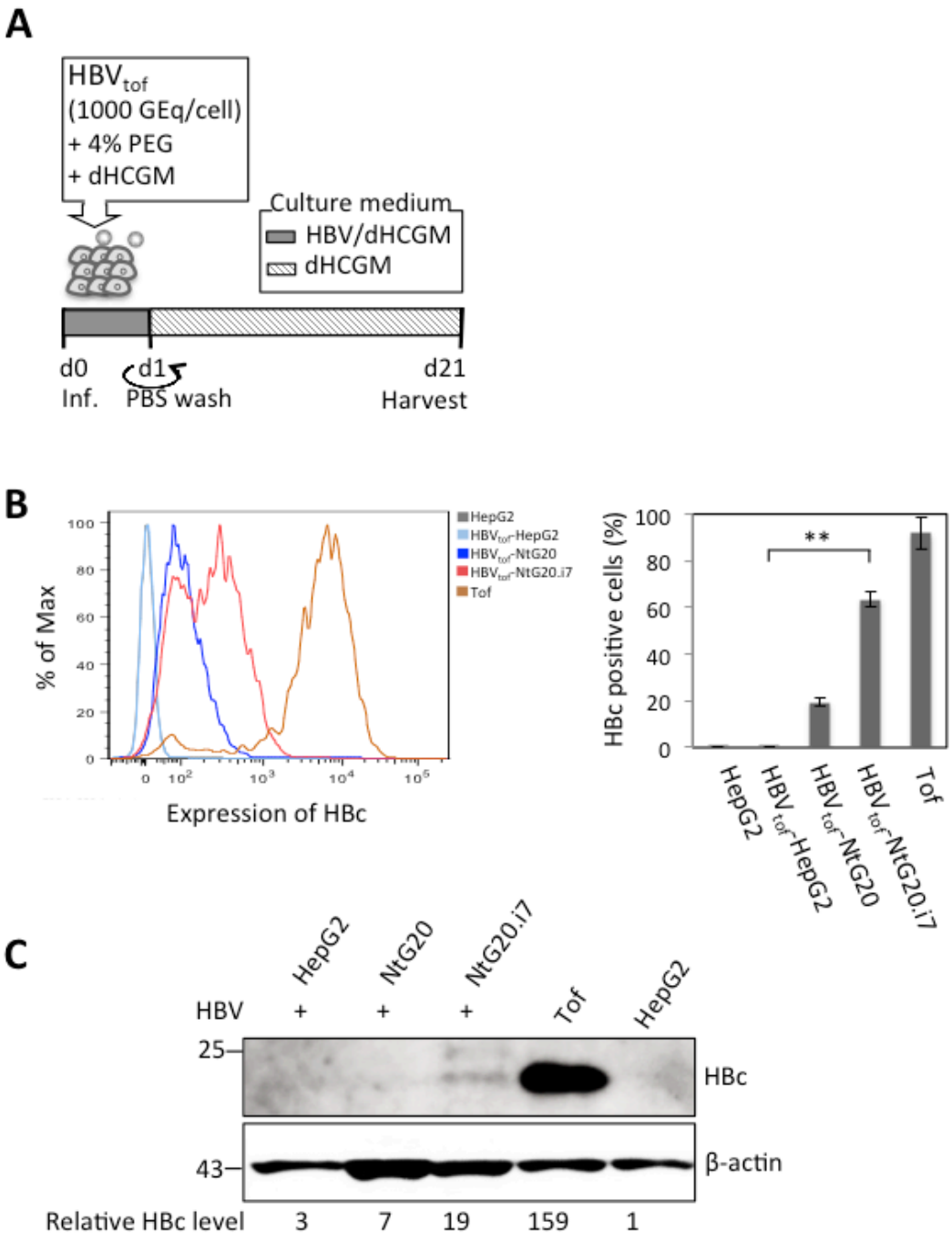
A
HBVtof
(1000 GEq/cell)
+ 4% PEG
+ dHCGM
Culture medium
HBV/dHCGM
dHCGM
d0
Inf.
d1
PBS wash
d21
Harvest
B
% of Max
Expression of HBc
HepG2
HBVtof-HepG2
HBVtof-NtG20
HBVtof-NtG20.i7
Tof
HBc positive cells (%)
**
HepG2
HBVtof-HepG2
HBVtof-NtG20
HBVtof-NtG20.i7
Tof
C
HepG2
NtG20
NtG20.i7
Tof
HepG2
HBV
+
+
+
25
HBc
43
β-actin
Relative HBc level
3
7
19
159
1

Fig. 4. HBV infection in HepG2 and its derivative cell lines

(A) Scheme of HBV infection. Condensed culture medium of Hep38.7-Tet cells was used as the inoculum (HBV_{tof}). Virus adsorption and subsequent culture maintenance were performed as indicated. (B) Analysis of HBc expression at 21 dpi. A portion of non-infected (mock) or HBV_{tof}-infected HepG2, NtG20, and NtG20.i7 cells were fixed and permeabilized, then examined by FACS using an anti-HBc antibody. Hep38.7-Tof cells were examined for comparison. The percentage of HBc-positive cells was quantified, as shown in the right panel. (C) The infected cells were subjected to immunoblot analysis using an anti-HBc antibody. β-actin served as a loading control. The bands corresponding to HBc were quantified and relative levels were calculated using β-actin as standard control (bottom).

Figure 5

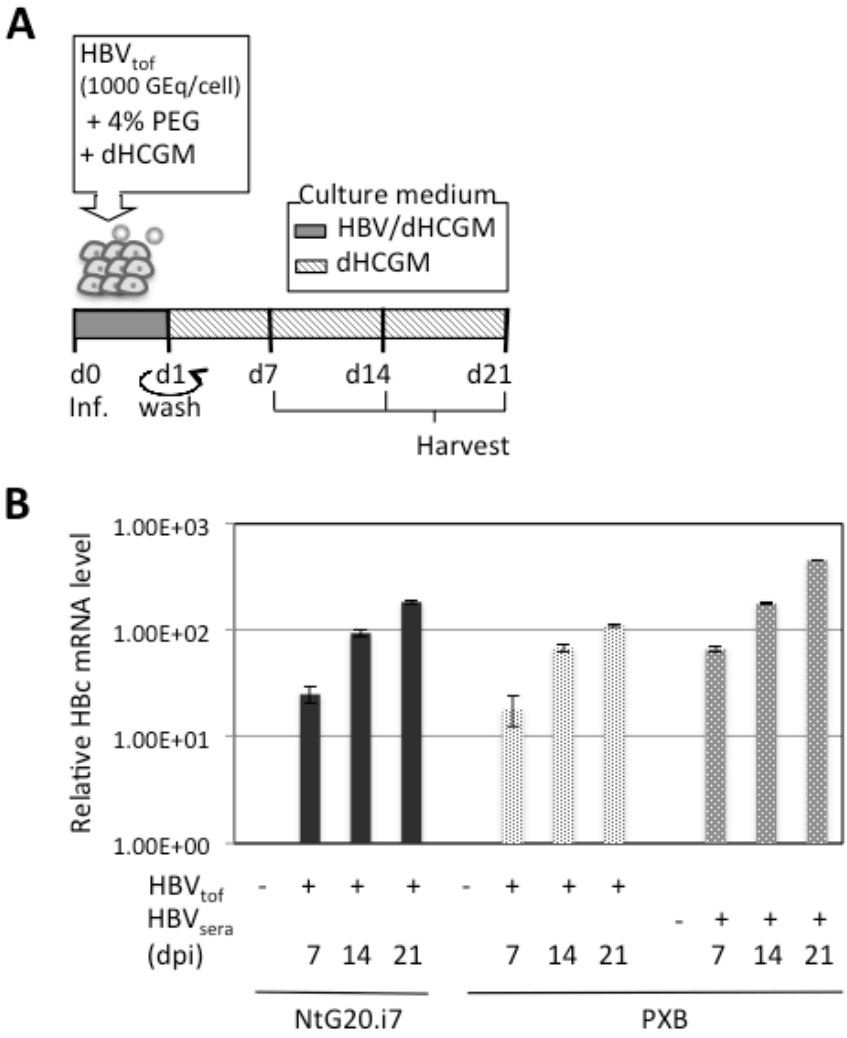
A
HBVtof
(1000 GEq/cell)
+ 4% PEG
+ dHCGM
Culture medium
HBV/dHCGM
dHCGM
d0
Inf.
d1
wash
d7
d14
d21
Harvest
B
Relative HBc mRNA level
1.00E+03
1.00E+02
1.00E+01
1.00E+00
HBVtof
HBVsera
(dpi)
NtG20.i7
PXB
C
Mock
HBVtof-NtG20.i7
HBVtof-PXB
Tof
25
43
HBc
β-actin

Fig. 5. HBV infection in NtG20.i7 and PXB cells

(A) Scheme of HBV infection in NtG20.i7 and PXB cells at various time points. PXB cells were exposed to HBV_{sera} as a positive control of HBV infection. (B) Intracellular mRNA levels of HBc were examined by real-time PCR. (C) Examination of HBc expression in the cell lysate of HBV_{tof}-infected NtG20.i7 and PXB cells at 21 dpi by immunoblotting. β-actin served as a loading control.

Figure 6

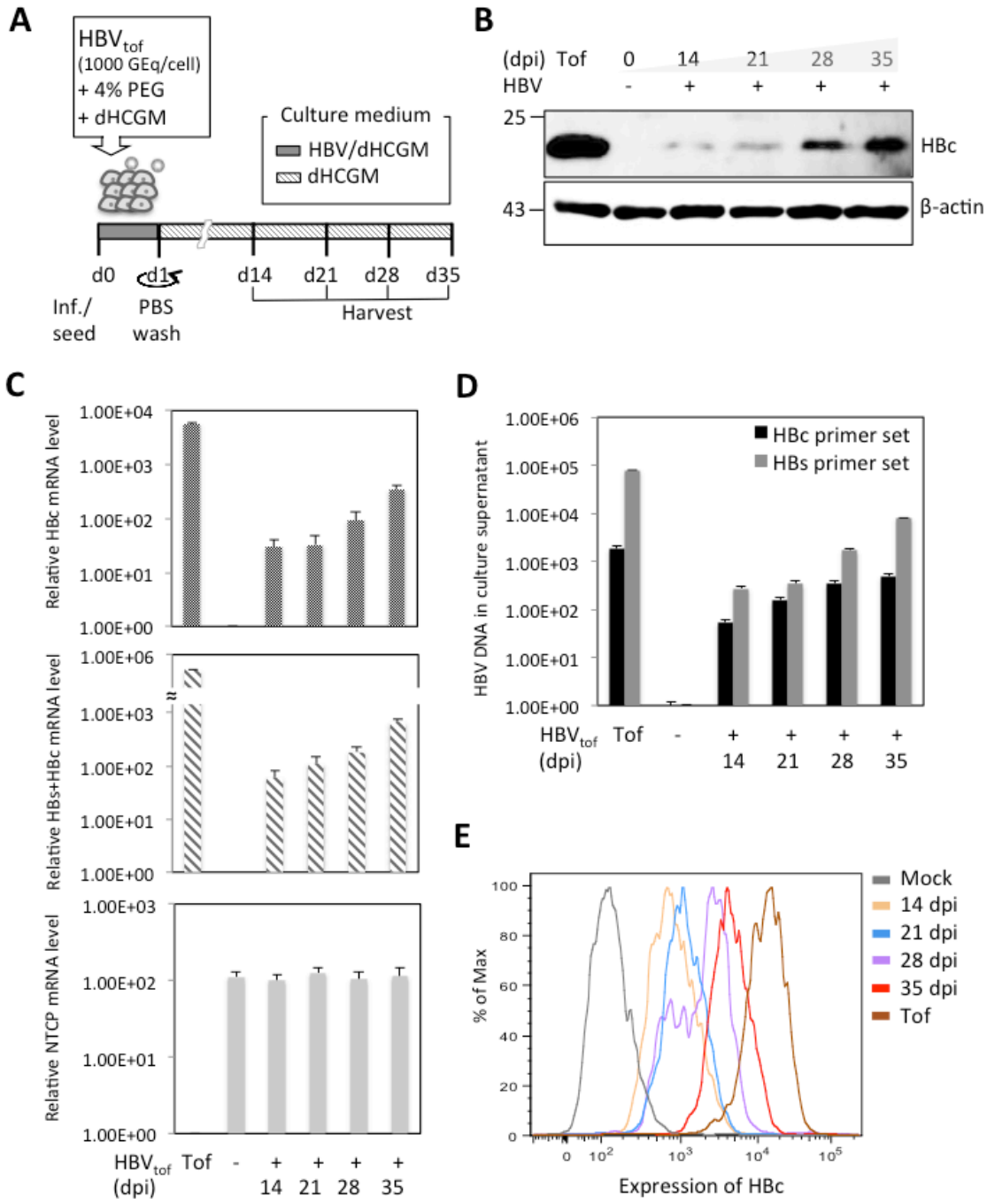
A
HBVtof
(1000 GEq/cell)
+ 4% PEG
+ dHCGM
Culture medium
HBV/dHCGM
dHCGM
d0
d1
d14
d21
d28
d35
Inf./
seed
PBS
wash
Harvest
B
(dpi) Tof 0 14 21 28 35
HBV - + + + +
25
43
HBc
β-actin
C
Relative HBc mRNA level
Relative HBs+HBc mRNA level
Relative NTCP mRNA level
1.00E+00
1.00E+01
1.00E+02
1.00E+03
1.00E+04
1.00E+06
HBVtof Tof - + + + +
(dpi) 14 21 28 35
D
HBV DNA in culture supernatant
1.00E+00
1.00E+01
1.00E+02
1.00E+03
1.00E+04
1.00E+05
1.00E+06
HBc primer set
HBs primer set
HBVtof Tof - + + + +
(dpi) 14 21 28 35
E
% of Max
0
20
40
60
80
100
0 10^2 10^3 10^4 10^5
Expression of HBc
Mock
14 dpi
21 dpi
28 dpi
35 dpi
Tof

Fig. 6. Long-term maintenance of HBV replication in NtG20.i7 cells

(A) NtG20.i7 cells were infected with HBV derived from Hep38.7-Tet cells, as indicated. The infected cells and culture media were harvested at various indicated time points for further examinations. (B) Intracellular HBc expression examined by immunoblotting using antibodies for HBc and β-actin. Hep38.7-Tet cells cultured in the absence of tetracycline (Tof) were examined as a positive control. (C) Intracellular mRNA levels of HBc, HBs, and NTCP were examined by real-time PCR. (D) HBV DNA in the culture supernatant was extracted by smi-TEST and quantified by real-time PCR for specific primer sets for HBc and HBs. (E) Examination for intracellular HBc expression by FACS.

Figure 7

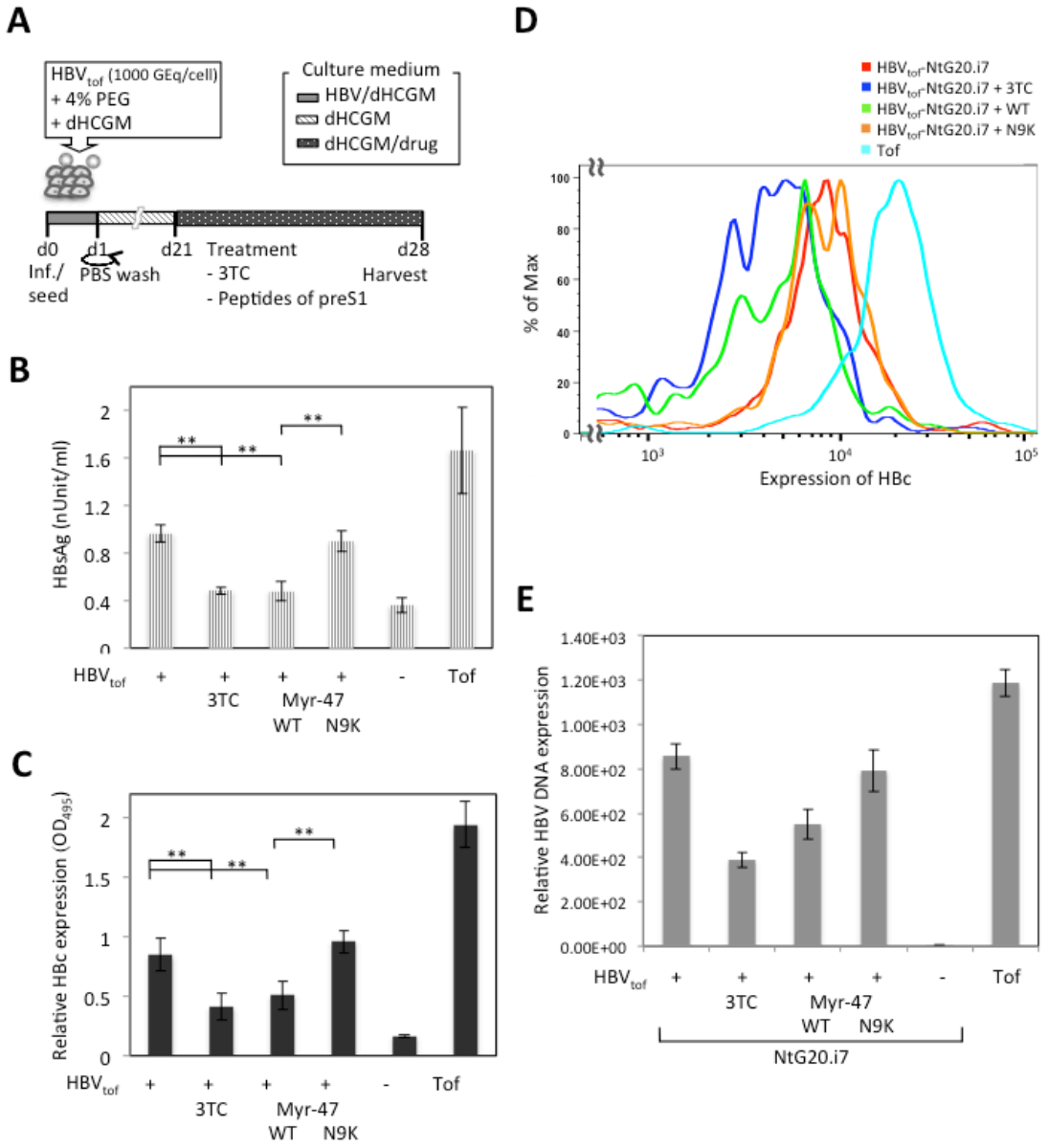
A
HBVtof (1000 GEq/cell)
+ 4% PEG
+ dHCGM
Culture medium
HBV/dHCGM
dHCGM
dHCGM/drug
d0
Inf./
seed
d1
PBS wash
d21
Treatment
- 3TC
- Peptides of preS1
d28
Harvest
B
HBsAg (nUnit/ml)
HBVtof
3TC
Myr-47
WT
N9K
Tof
C
Relative HBc expression (OD495)
D
HBVtof-NtG20.i7
HBVtof-NtG20.i7 + 3TC
HBVtof-NtG20.i7 + WT
HBVtof-NtG20.i7 + N9K
Tof
% of Max
Expression of HBc
E
Relative HBV DNA expression
NtG20.i7

Fig. 7. *De novo* HBV infection during long-term culture of NtG20.i7 cells

(A) Scheme of HBV infection in NtG20.i7 cells. Cells were infected for 21 days and mock treated, treated with 3TC (50 mM), preS1 peptide (WT, 200 nM), or mutant preS1 peptide (N9K, 200 nM), as indicated. At 28 days post infection, cells were harvested. (B) HBsAg in the culture supernatant was determined by ELISA. Tof: Hep38.7-Tet culture supernatant without adding tetracycline. (C) Cells in 96-well plates were fixed, permeabilized, and subjected to microplate immunostaining for HBc (Materials and Methods). Tof: Hep38.7-Tet cells cultured in the absence of tetracycline. (D) To address antiviral treatments in HBV-infected NtG20.i7 cells, cells were subjected to 3TC and peptides of preS1 (WT and N9K) treatment for 7 days and then harvested to examine viral products. HBcAg level in these cells was quantified by FACS analysis. (E) Relative HBV DNA expression level was examined.

** $p < 0.01$, *** $p < 0.001$

Figure 8

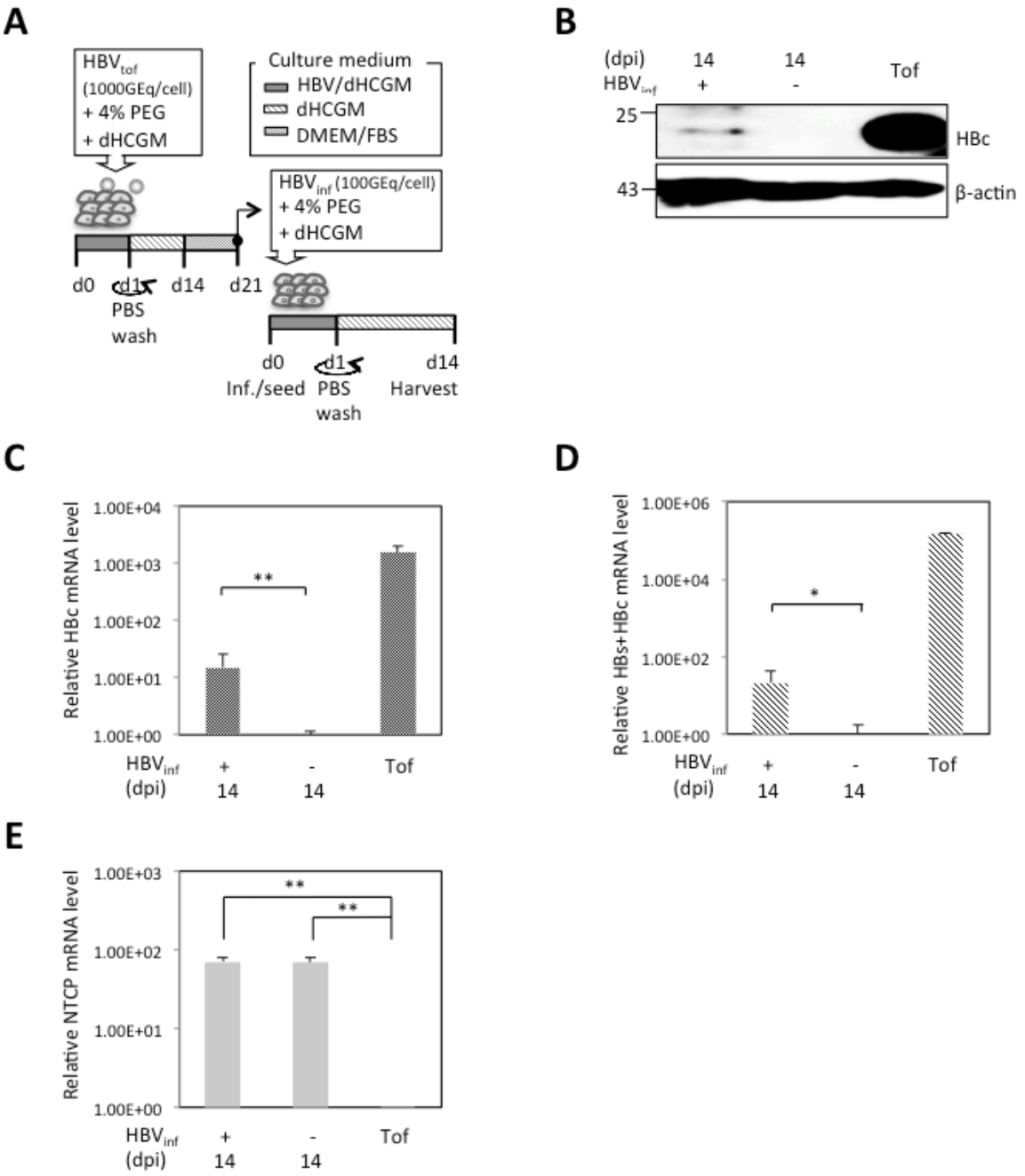
A
HBVtof (1000GEq/cell) + 4% PEG + dHCGM
Culture medium
HBV/dHCGM
dHCGM
DMEM/FBS
HBVinf (100GEq/cell) + 4% PEG + dHCGM
d0
d1
d14
d21
PBS wash
d0
d1
d14
Inf./seed
PBS wash
Harvest
B
(dpi)
HBVinf
14
14
Tof
+
-
25
43
HBc
β-actin
C
Relative HBc mRNA level
1.00E+04
1.00E+03
1.00E+02
1.00E+01
1.00E+00
**
HBVinf
(dpi)
+
14
-
14
Tof
D
Relative HBs+HBc mRNA level
1.00E+06
1.00E+04
1.00E+02
1.00E+00
*
HBVinf
(dpi)
+
14
-
14
Tof
E
Relative NTCP mRNA level
1.00E+03
1.00E+02
1.00E+01
1.00E+00
**
**
HBVinf
(dpi)
+
14
-
14
Tof

Fig. 8. Re-infection in fresh NtG20.i7 cells

(A) Scheme of re-infection. The culture supernatant of HBV_{tof}-infected NtG20.i7 cells was harvested at 21 dpi, and is indicated as HBV_{inf}. Fresh NtG20.i7 cells subjected to the HBV_{inf} at 100 GEq/cell, which had been condensed by 20-fold. (B) Examination of HBc expression re-infection by immunoblotting. β-actin served as a loading control. Tof: Hep38.7-Tet cells cultured in the absence of tetracycline. At 14 dpi, cellular RNA was extracted and quantified for HBc (C), HBs (D), and NTCP mRNA(E) by real-time PCR.

Figure 9

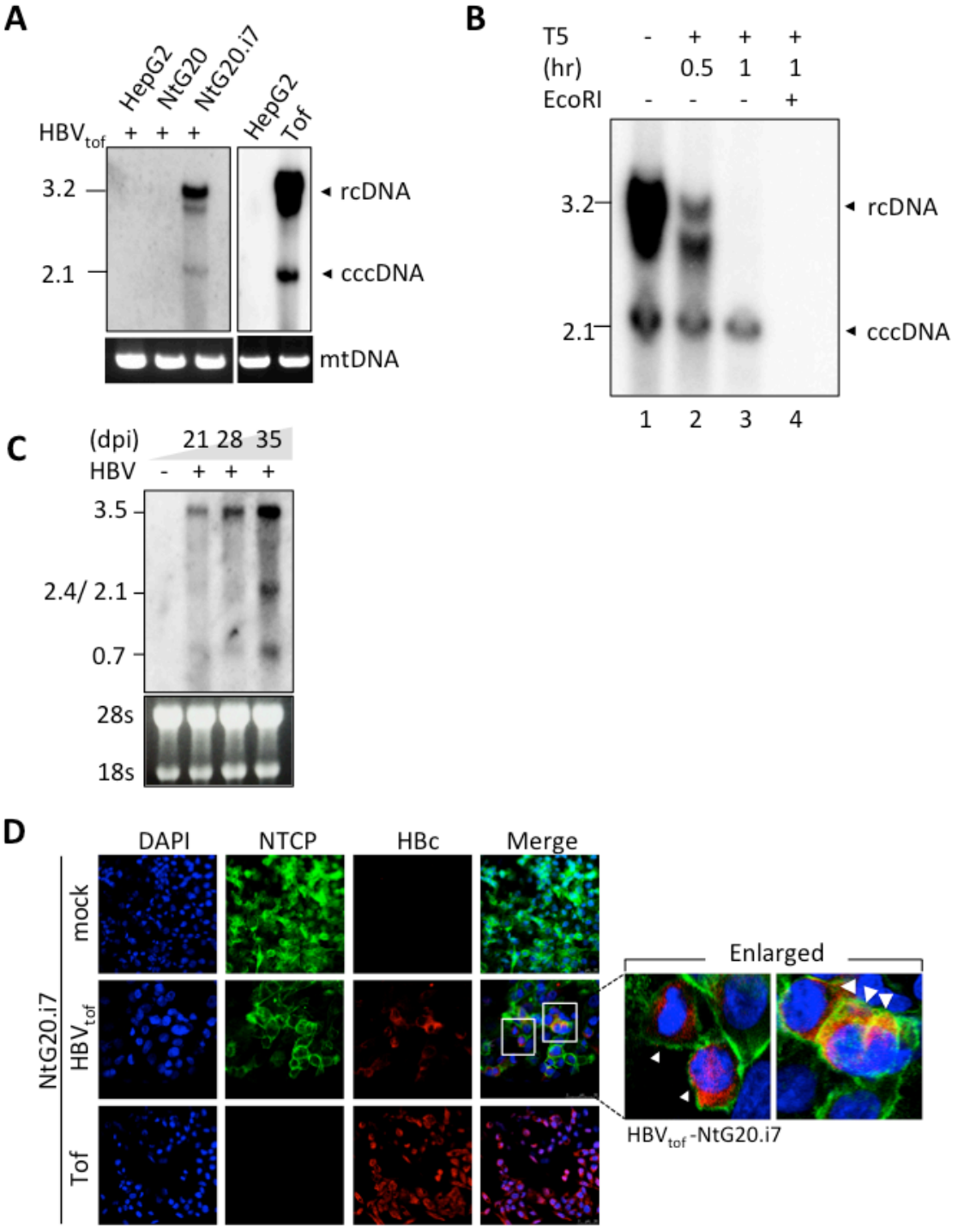
A
HepG2
NtG20
NtG20.i7
HepG2
Tof
HBVtof + + +
3.2
2.1
rcDNA
cccDNA
mtDNA
B
T5 - + + +
(hr) 0.5 1 1
EcoRI - - - +
3.2
2.1
rcDNA
cccDNA
1 2 3 4
C
(dpi) 21 28 35
HBV - + + +
3.5
2.4/ 2.1
0.7
28s
18s
D
DAPI
NTCP
HBc
Merge
NtG20.i7
mock
HBVtof
Tof
Enlarged
HBVtof-NtG20.i7

Fig. 9. HBV replication in NtG20.i7 cells

NtG20.i7 cells were infected with HBV for 35 days, as described in Fig. 8. (A) DNA was extracted by the Hirt method and subjected to Southern blotting using HBV sequence as the probe. Positions of rcDNA and cccDNA are indicated. (B) Validation of cccDNA detection in HBV-infected NtG20.i7 cells. Hirt DNA extracted from HBV-infected NtG20.i7 cells (5×10^6 cells) was mock treated (-) or treated (+) with T5 nuclease (10 units) for 30 min or 1 hr at 37℃, as indicated, then subjected to Southern blotting using HBV sequence as the probe. The fast migrating DNA (corresponding to the 2.1 kbp marker position) is more resistant compared to rcDNA (at the 3.2 kbp marker position, lanes 1-3). EcoRI digestion, which converts cccDNA into linear dsDNA, eliminated cccDNA detection after T5 digestion (lane 4). These results suggest that the band migrating at the 2.1 kbp position corresponds to cccDNA. (C) NtG20.i7 cells were infected with HBV for 28 days and immunostained for HBc (Red). Nuclei staining with DAPI (Blue). NTCP: tGFP fluorescence (Green). Tof: Hep38.7-Tet cells cultured in the absence of tetracycline. Arrows indicate HBc-positive cells.

Figure 10

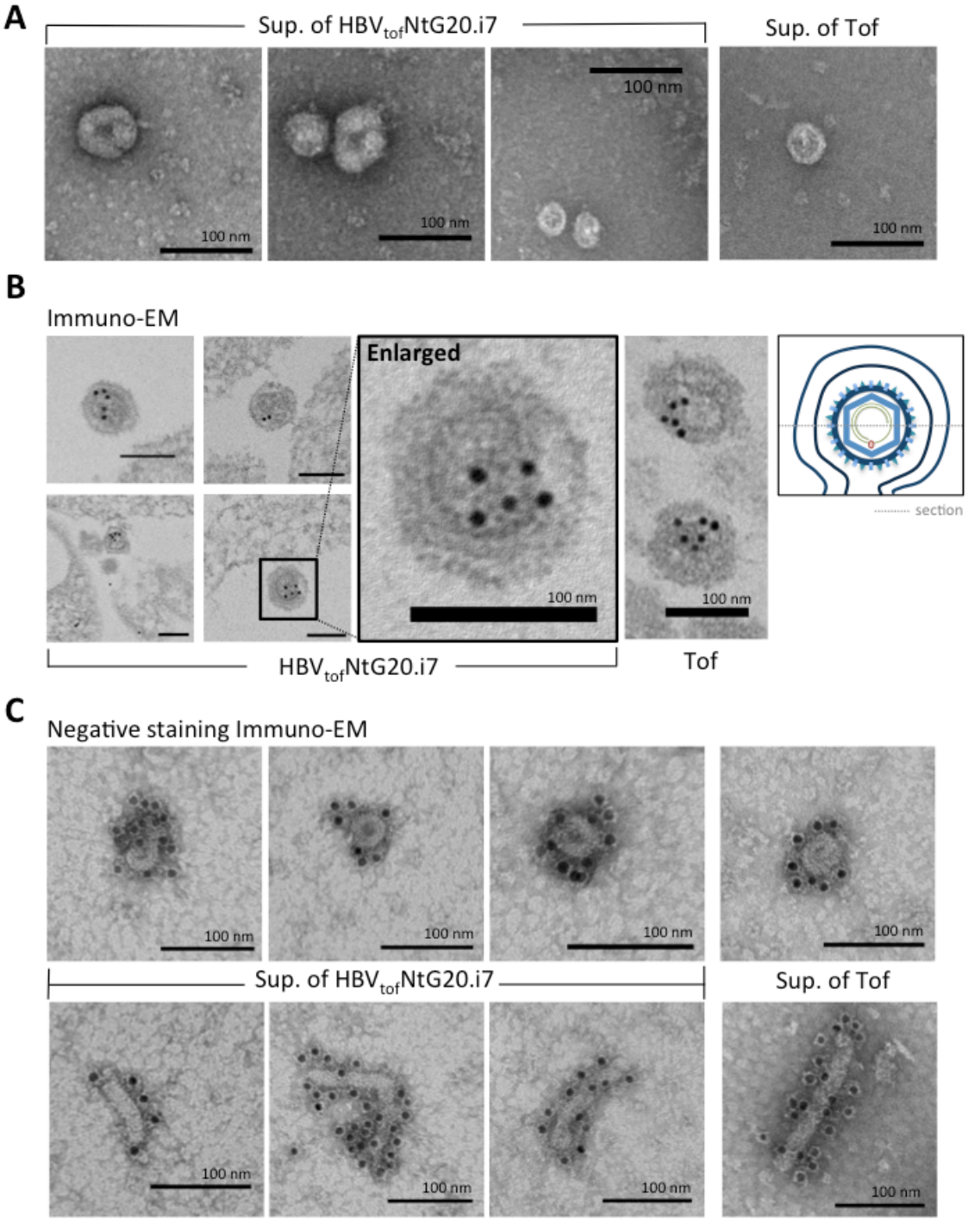
A
Sup. of HBV$_{tof}$NtG20.i7
Sup. of Tof
100 nm
B
Immuno-EM
Enlarged
section
HBV$_{tof}$NtG20.i7
Tof
C
Negative staining Immuno-EM
Sup. of HBV$_{tof}$NtG20.i7
Sup. of Tof

Fig. 10. Virion and subviral particle in HBV-infected NtG20.i7 cells

(A) The supernatant of NtG20.i7 cells infected with HBV for 28 days were ultra-centrifuged to condensation. After CsCl gradient fractionation, the infected medium were subjected to detect by EM. Scale bar = 100 nm. (B) The infected cells were fixed and processed for ultrasectioning and examined by immuno-EM by HBc antibody. Tof: Hep38.7 indicated as a positive control. Scale bar = 100 nm. Right: schematic image of intracellular virion surrounded by ER and plasma membranes. (C) Inoculum from Tof and the culture supernatant of infected NtG20.i7 cells were subjected to CsCl gradient fractionation. Fractions containing both HBs and HBV DNA were examined by negative-staining immuno-EM analysis with HBs antibody. Moreover, culture supernatant was harvested from infected cells at 21 dpi and Hep38.7-Tet at day 6 after removal of tetracycline. Negative-staining immuno-EM was performed with HBs antibody. HBs-positive, filament-like structures with an approximate diameter of 22 nm were observed. Scale bar = 100 nm.

Materials and Methods

Cell Culture.

Cells were maintained in Dulbecco's Modified Eagle's Medium with 10% fetal bovine serum, 100 U/mL Penicillin and 100 μg/mL streptomycin (common medium) at 37°C in a 5% CO_2 incubator. ES2 cells, which stably express 1.3-fold HBV genome, constitutively produce infectious HBV in the culture supernatant [64]. Hep38.7-Tet cells, established by Naoki Ogura [54], produce infectious HBV in a tetracycline-suppressive manner. Hep38.7-Tet cells were maintained in the common medium in the presence of tetracycline (400 ng/ml). NtG20 cells, stably expressing human NTCP, were cultured in common medium with 500 μg/mL G418. NtG20.i7 cells, a stable cell line expressing human NTCP with a knockdown of IPS-1, were maintained in common medium with 400 μg/ml G418 and 100 μg/ml Hygromycin B.

Plasmids and Transfection.

HepG2 cells stably expressing human NTCP-turbo GFP (tGFP) fusion were established by transfecting an expression vector for human NTCP (NM_003049, Human cDNA ORF Clone, ORIGENE) C-terminally fused with tGFP using Lipofectamine 2000 (Life technologies) and selected using G418 (500 μg/mL). Cells

expressing NTCP-tGFP were selected by FACS sorting and several clones were obtained. One of the clones, NtG20, was finally chosen due to its high NTCP expression. Using NtG20, we further selected a clone that could stably knockdown IPS-1 by transfecting a shRNA construct, psiRNA-h7SK (InvivoGen), and using Hygromycin B (100 μg/mL). The cells were cloned for stable expression of NTCP-tGFP and knockdown for IPS-1. One of the clones, NtG20.i7, was finally selected.

RNA Interference.

The synthetic siRNA for negative controls (Invitrogen, Cat. No. 1293-112), IPS-1 (Invitrogen, Cat. No. BS-D20), and STING (Bonac Corporation 5122418) were transfected into ES2 cells with RNAi MAX (Invitrogen) and cultivated with optiMEM according to the manufacturer's instructions.

RNA extraction and Real-time PCR.

Total RNA was isolated with TRIzol (Invitrogen) and reverse transcribed using a TaqMan MicroRNA Reverse Transcription Kit to produce cDNA. Real-time PCR (RT-PCR) for NTCP and HBV core and surface (base on accession number of HBV genome: AB644287) were performed using a Fast SYBR Green Master Mix (Applied

Biosystems) according to the manufacturer's protocol. The human GAPDH gene was used as an internal control to normalize differences in each sample. The sequences of primers were:

HBV core (HBc) forward, 5'-TTCACCTCACCATACAGCACTC-3'

HBc reverse, 5'-ATAGGGGCATTTGGTGGTCTG-3'

HBV surface (HBs) forward, 5'-AATCCTCACAATACCGCAGA-3'

HBs reverse, 5'-AGGCATAGCAGCAGGATGAA-3'

GAPDH forward, 5'-TGCACCACCAACTGCTTAGC-3'

GAPDH reverse, 5'-GGCATGGACTGTGGTCATGAG-3'

NTCP forward, 5'- AGTTCAGCAAGATCAAGGCT-3'

NTCP reverse, 5'- ATGGCCAGACTGAAGACATT-3'

HBV Infection.

The culture medium of Hep38.7-Tet cells was used for HBV inoculum. Hep38.7-Tet cells were seeded with tetracycline, and after 1 day of cultivation the cells were washed and cultivated for 6 more days in the absence of tetracycline. The supernatant was harvested and concentrated using a Centricon (Millipore) to 1/20 of the original volume. Cells were seeded in 6 well plates at 10^5 cells/well with dHCGM [19]

containing condensed HBV and PEG 8000 (4%) for 24 hr. The next day, the medium was replaced with fresh dHCGM.

Enzyme-Linked Immunosorbent Assay (ELISA).

Culture supernatants were analyzed using HBs ELISA (Beacle, Inc.) according to the manufacturer's protocol.

Detection of viral release.

DNA was extracted from culture supernatant using SMI-TEST EX-R&D (MEDICAL & BIOLOGICAL LABORATORIES CO., LTD) according to the manufacturer's protocol. All extracted DNA were dissolved in nuclease-free water and quantified by RT-PCR using HBc and HBs primer sets, respectively.

Immunofluorescence Microscopy and Fluorescence Imaging.

HBV-infected hepatocytes were fixed with 4% paraformaldehyde (PFA) for 15 min at 4°C and then washed 3 times with PBS. Cells were permeabilized with 0.05% Triton X-100 in PBS for 10 min at room temperature, blocked with 5 mg/ml BSA in PBST (0.04% Tween20 in PBS) for 30 min, and incubated with the targeting primary antibody diluted in blocking buffer at 4°C overnight. Following this, cells were incubated with secondary antibodies at room temperature for 1 hr, then nuclei were

stained with 4.6-dimaidino-2-phenylinodole (DAPI) and observed using a confocal laser microscope, TCS-SP (Leica).

Immunoblotting.

Immunoblotting was performed as described previously [65]. Proteins were visualized by chemical luminescence using secondary antibodies conjugated with horseradish peroxidase (HRP). Antibodies used were: HBcAg (rabbit anti-HBcAg, Neomarkers, 1413R810A, Fremont, CA, USA), IPS-1 (rabbit anti-MAVS, Abcam ab25084), STING (rabbit, hMITA275-92, Immuno-Biological Laboratories Co,Ltd, Japan), NTCP (rabbit anti-SLC10A1, Atlas antibody, HPA042727, Sweden), and beta-actin (Sigma, Cat. No. A8481).

Flow cytometry analysis.

Cells were detached from the culture dish by trypsin and fixed with 1% PFA for 15 min at room temperature, then washed with PBS 3 times. Cells were permeabilized with 0.05% Triton X-100 in PBS for 10 min at room temperature, blocked with 10% Donkey serum in PBS for 30 min, and incubated with the targeting primary antibody overnight at 4°C. Cells were washed with FACS buffer (HBSS(+), 0.02% BSA, and 0.05%NaN_3) and then incubated with Alexa 647-conjugated IgG secondary antibody in

FACS buffer at room temperature for 1 hr. Cells were washed and then subjected to analysis by flow cytometry.

Microplate immunostaining for HBc.

Cells were seeded in 96-well plates and then fixed with 4% PFA for 15 min at room temperature. Cells were then washed with PBS 3 times, permeabilized with 0.05% Triton X-100 in PBS for 10 min at room temperature, blocked with 10% Donkey serum in PBS for 30 min, and incubated with the targeting primary antibody diluted in blocking buffer at 4°C overnight. Cells were washed with TBST and then incubated with HRP-conjugated IgG secondary antibody at room temperature for 1 hr. After carefully washing with TBST, a TMB mixture (ELISA POD Substrate TMB Kit) was added to the plate to visualize the signal. After termination of the reaction by adding acid buffer, signals were quantified by photometer at an absorbance of 450 nm.

Southern blot.

The HBV DNA probe was synthesized using a Random Primer DNA Labeling Kit (Takara). All extracted DNA samples underwent southern blotting analysis as previously described [58]. Steps were carried out in accordance with the manufacturer's protocol. Signals were visualized and analyzed using the FUJIFILM

BAS-5000 image scanner.

CsCl gradient fractionation.

CsCl density gradients (15 ml) ranging from 5 to 40% (w/w) in TNE (10mM Tris-HCl pH7.6, 150 mM NaCl, 1mM EDTA) were prepared using The Gradient Station (Biocomp). 500 μl of concentrated culture medium from Hep38.7-Tet and i7 cells were carefully loaded onto the top of the gradient and centrifuged for 16 hour at 28,000 rpm in a P28S2 swing rotor (HITACHI) at 15°C. 24 fractions were collected using The Gradient Station and AC-5700P Micro Collector (ATTO), and HBs antigen and HBV-DNA levels in each fraction were analyzed by ELISA and qPCR, respectively. Fractions positive for HBs and HBV-DNA were dialyzed by the Oscillatory Microdialysis System (Bio-Tech), and subjected to electron microscopy.

Ultrathin-section immuno-EM.

Cells were fixed with 4% paraformaldehyde and 2% glutaraldehyde overnight at 4°C [66]. Then, cells were incubated with 0.5% osmium tetroxide in 0.1M phosphate buffer for 40 min at room temperature. After dehydration with ethanol, cells were embedded in epoxy resin (Luveak; Nacalai Tesque, Japan). Once the resin was polymerized, the cells were cut into ultrathin sections on an ultramicrotome, EM UC7 (Leica). Sections

of the sample (50 nm-thick) were etched on nickel grids with saturated sodium periodate solution [67], washed with PBS, and treated with the blocking solution. The grids were then incubated with an anti-HBc mouse monoclonal antibody. After being washed with PBS, they were incubated with a goat anti-mouse immunoglobulin conjugated to 10-nm gold particles. The samples were washed, fixed with 1% GLA, and stained with 2% UA and Reynolds lead. The digital images were recorded with a TEM operated at 80 kV.

Negative-staining immuno-EM.

Supernatants were adsorbed to Formvar-coated nickel grids and prefixed with 4% paraformaldehyde phosphate buffer solution (WAKO). The grids were washed, treated with blocking solution (Blocking One; Nacalai Tesque.), and then incubated with an anti-HBs rabbit antibody. After being washed with PBS, they were incubated with a goat anti-rabbit immunoglobulin conjugated to 10-nm gold particles (BBI Solutions). The samples were washed, fixed with 1% GLA, and negatively stained with 2% uranyl acetate solution (UA). The images were recorded using an HT7700 transmission electron microscope (TEM) (Hitachi) operated at 80 kV

Statistical analysis.

All experimental values are presented as the mean ± standard error for at least 3 independent recordings. Data were analyzed using Statistical Product and Service Solutions software and EXCEL.

Bibliography

1. Ganem D, Prince AM: Hepatitis B virus infection--natural history and clinical consequences. *N Engl J Med* 2004, 350:1118-1129.
2. Chan KM, Yam I, Yuen J, Yuen MF, Lai CL, Alexander GJ, Chan TK, Chan V: A comprehensive HBV array for the detection of HBV mutants and genotype. *Clinical Biochemistry* 2011, 44:1253-1260.
3. Congly SE, Wong P, Al-Busafi SA, Fung SK, Ghali P, Betel M, Fonseca K, Myers RP, Osiowy C, Coffin CS: Characterization of Hbv Genotype Epidemiology and Hbsag Titres in Response to Anti-Hbv Antiviral Therapy in Canadian Tertiary Referral Liver Centres. *Hepatology* 2011, 54:893A-893A.
4. Lavanchy D: Hepatitis B virus epidemiology, disease burden, treatment, and current and emerging prevention and control measures. *J Viral Hepat* 2004, 11:97-107.
5. Sharma S, Carballo M, Feld JJ, Janssen HLA: Immigration and viral hepatitis. *Journal of Hepatology* 2015, 63:515-522.
6. Pollicino T, Raimondo G: Occult Hepatitis B Infection. *Journal of Hepatology* 2014, 61:688-689.
7. Protzer U, Maini MK, Knolle PA: Living in the liver: hepatic infections. *Nat Rev Immunol* 2012, 12:201-213.
8. Chisari FV, Isogawa M, Wieland SF: Pathogenesis of hepatitis B virus infection. *Pathol Biol (Paris)* 2010, 58:258-266.
9. Chang JH, Block TM, Guo JT: The innate immune response to hepatitis B virus infection: Implications for pathogenesis and therapy. *Antiviral Research* 2012, 96:405-413.
10. Zoulim F: Are novel combination therapies needed for chronic hepatitisB ? *Antiviral Res* 2012, 96:256-259.
11. Hatzakis A, Magiorkinis E, Haida C: HBV virological assessment. *Journal of Hepatology* 2006, 44:S71-S76.
12. Mhamdi M, Funk A, Hohenberg H, Will H, Sirma H: Assembly and budding of a hepatitis B virus is mediated by a novel type of intracellular vesicles. *Hepatology* 2007, 46:95-106.
13. Urban S, Schulze A, Dandri M, Petersen J: The replication cycle of hepatitis B

virus. *Journal of Hepatology* 2010, 52:282-284.
14. Patient R, Hourioux C, Sizaret PY, Trassard S, Sureau C, Roingeard P: Hepatitis B virus subviral envelope particle morphogenesis and intracellular trafficking. *J Virol* 2007, 81:3842-3851.
15. Trepo C, Chan HL, Lok A: Hepatitis B virus infection. *Lancet* 2014, 384:2053-2063.
16. Ezzikouri S, Ozawa M, Kohara M, Elmdaghri N, Benjelloun S, Tsukiyama-Kohara K: Recent Insights into Hepatitis B Virus-Host Interactions. *Journal of Medical Virology* 2014, 86:925-932.
17. Guidotti LG, Isogawa M, Chisari FV: Host-virus interactions in hepatitis Bvirus infection. *Current Opinion in Immunology* 2015, 36:61-66.
18. Tateno C, Yoshizane Y, Saito N, Kataoka M, Utoh R, Yamasaki C, Tachibana A, Soeno Y, Asahina K, Hino H, et al.: Near completely humanized liver in mice shows human-type metabolic responses to drugs. *Am J Pathol* 2004, 165:901-912.
19. Yamasaki C, Tateno C, Aratani A, Ohnishi C, Katayama S, Kohashi T, Hino H, Marusawa H, Asahara T, Yoshizato K: Growth and differentiation of colony-forming human hepatocytes in vitro. *J Hepatol* 2006, 44:749-757.
20. Tsuge M, Takahashi S, Hiraga N, Fujimoto Y, Zhang Y, Mitsui F, Abe H, Kawaoka T, Imamura M, Ochi H, et al.: Effects of hepatitis B virus infection on the interferon response in immunodeficient human hepatocyte chimeric mice. *J Infect Dis* 2011, 204:224-228.
21. Cui XJ, Clark DN, Liu KC, Xu XD, Guo JT, Hu JM: Viral DNA-Dependent Induction of Innate Immune Response to Hepatitis B Virus in Immortalized Mouse Hepatocytes. *Journal of Virology* 2016, 90:486-496.
22. Leong CR, Oshiumi H, Okamoto M, Azuma M, Takaki H, Matsumoto M, Chayama K, Seya T: A MAVS/TICAM-1-independent interferon-inducing pathway contributes to regulation of hepatitis B virus replication in the mouse hydrodynamic injection model. *J Innate Immun* 2015, 7:47-58.
23. Luangsay S, Ait-Goughoulte M, Michelet M, Floriot O, Bonnin M, Gruffaz M, Rivoire M, Fletcher S, Javanbakht H, Lucifora J, et al.: Expression and functionality of Toll- and RIG-like receptors in HepaRG cells. *J Hepatol* 2015, 63:1077-1085.
24. Gatanaga H, Hayashida T, Tanuma J, Oka S: Prophylactic effect of antiretroviral therapy on hepatitis B virus infection. *Clin Infect Dis* 2013, 56:1812-1819.

25. Halegoua-De Marzio D, Hann HW: Then and now: the progress in hepatitis B treatment over the past 20 years. *World J Gastroenterol* 2014, 20:401-413.
26. Gupta N, Goyal M, Wu CH, Wu GY: The Molecular and Structural Basis of HBV-resistance to Nucleos(t)ide Analogs. *J Clin Transl Hepatol* 2014, 2:202-211.
27. Baumert TF, Verrier ER, Nassal M, Chung RT, Zeisel MB: Host-targeting agents for treatment of hepatitis B virus infection. *Current Opinion in Virology* 2015, 14:41-46.
28. Locarnini S, Hatzakis A, Chen DS, Lok A: Strategies to control hepatitis B: Public policy, epidemiology, vaccine and drugs. *J Hepatol* 2015, 62:S76-86.
29. Hagenbuch B, Dawson P: The sodium bile salt cotransport family SLC10. *Pflugers Arch* 2004, 447:566-570.
30. Yan H, Zhong GC, Xu GW, He WH, Jing ZY, Gao ZC, Huang Y, Qi YH, Peng B, Wang HM, et al.: Sodium taurocholate cotransporting polypeptide is a functional receptor for human hepatitis B and D virus. *Elife* 2012, 1.
31. Yan H, Liu Y, Sui J, Li W: NTCP opens the door for hepatitis B virus infection. *Antiviral Res* 2015, 121:24-30.
32. Anwer MS, Stieger B: Sodium-dependent bile salt transporters of the SLC10A transporter family: more than solute transporters. *Pflugers Arch* 2014, 466:77-89.
33. Elinger S: HBV: Stowaway of NTCP. *Clin Res Hepatol Gastroenterol* 2014, 38:661-663.
34. Konig A, Doring B, Mohr C, Geipel A, Geyer J, Glebe D: Kinetics of the bile acid transporter and hepatitis B virus receptor Na+/taurocholate cotransporting polypeptide (NTCP) in hepatocytes. *Journal of Hepatology* 2014, 61:867-875.
35. Watashi K, Urban S, Li W, Wakita T: NTCP and beyond: opening the door to unveil hepatitis B virus entry. *Int J Mol Sci* 2014, 15:2892-2905.
36. Sun Y, Qi Y, Peng B, Li W: NTCP-Reconstituted In Vitro HBV Infection System. *Methods Mol Biol* 2017, 1540:1-14.
37. Li H, Zhuang QY, Wang YZ, Zhang TY, Zhao JH, Zhang YL, Zhang JF, Lin Y, Yuan Q, Xia NS, et al.: HBV life cycle is restricted in mouse hepatocytes expressing human NTCP. *Cellular & Molecular Immunology* 2014, 11:175-183.
38. Iwamoto M, Watashi K, Tsukuda S, Aly HH, Fukasawa M, Fujimoto A, Suzuki R, Aizaki H, Ito T, Koiwai O, et al.: Evaluation and identification of hepatitis B virus entry inhibitors using HepG2 cells overexpressing a membrane

transporter NTCP. *Biochemical and Biophysical Research Communications* 2014, 443:808-813.
39. Tsukuda S, Watashi K, Iwamoto M, Suzuki R, Aizaki H, Okada M, Sugiyama M, Kojima S, Tanaka Y, Mizokami M, et al.: Dysregulation of Retinoic Acid Receptor Diminishes Hepatocyte Permissiveness to Hepatitis B Virus Infection through Modulation of Sodium Taurocholate Cotransporting Polypeptide (NTCP) Expression. *Journal of Biological Chemistry* 2015, 290:5673-5684.
40. Yan R, Zhang Y, Cai D, Liu Y, Cuconati A, Guo H: Spinoculation Enhances HBV Infection in NTCP-Reconstituted Hepatocytes. *PLoS One* 2015, 10:e0129889.
41. Marsili G, Perrotti E, Remoli AL, Acchioni C, Sgarbanti M, Battistini A: IFN Regulatory Factors and Antiviral Innate Immunity: How Viruses Can Get Better. *J Interferon Cytokine Res* 2016, 36:414-432.
42. Liu Y, Olagnier D, Lin R: Host and Viral Modulation of RIG-I-Mediated Antiviral Immunity. *Front Immunol* 2016, 7:662.
43. Yoneyama M, Kikuchi M, Natsukawa T, Shinobu N, Imaizumi T, Miyagishi M, Taira K, Akira S, Fujita T: The RNA helicase RIG-I has an essential function in double-stranded RNA-induced innate antiviral responses. *Nature Immunology* 2004, 5:730-737.
44. Kawai T, Takahashi K, Sato S, Coban C, Kumar H, Kato H, Ishii KJ, Takeuchi O, Akira S: IPS-1, an adaptor triggering RIG-I- and Mda5-mediated type I interferon induction. *Nat Immunol* 2005, 6:981-988.
45. Bamming D, Horvath CM: Regulation of signal transduction by enzymatically inactive antiviral RNA helicase proteins MDA5, RIG-I, and LGP2. *J Biol Chem* 2009, 284:9700-9712.
46. Li X, Ranjith-Kumar CT, Brooks MT, Dharmaiah S, Herr AB, Kao C, Li P: The RIG-I-like receptor LGP2 recognizes the termini of double-stranded RNA. *J Biol Chem* 2009, 284:13881-13891.
47. Rehermann B, Nascimbeni M: Immunology of hepatitis B virus and hepatitis C virus infection. *Nature Reviews Immunology* 2005, 5:215-229.
48. Revill P, Yuan ZH: New insights into how HBV manipulates the innate immune response to establish acute and persistent infection. *Antiviral Therapy* 2013, 18:1-15.
49. Busca A, Kumar A: Innate immune responses in hepatitis B virus (HBV) infection. *Virol J* 2014, 11:22.
50. Oh IS, Park SH: Immune-mediated Liver Injury in Hepatitis B Virus Infection.

Immune Netw 2015, 15:191-198.
51. Takeuchi O, Akira S: Toll-like receptors; their physiological role and signal transduction system. *International Immunopharmacology* 2001, 1:625-635.
52. Wu J, Meng Z, Jiang M, Pei R, Trippler M, Broering R, Bucchi A, Sowa JP, Dittmer U, Yang D, et al.: Hepatitis B virus suppresses toll-like receptor-mediated innate immune responses in murine parenchymal and nonparenchymal liver cells. *Hepatology* 2009, 49:1132-1140.
53. Ishikawa H, Ma Z, Barber GN: STING regulates intracellular DNA-mediated, type I interferon-dependent innate immunity. *Nature* 2009, 461:788-U740.
54. Ogura N, Watashi K, Noguchi T, Wakita T: Formation of covalently closed circular DNA in Hep38.7-Tet cells, a tetracycline inducible hepatitis B virus expression cell line. *Biochem Biophys Res Commun* 2014, 452:315-321.
55. Ishida Y, Yamasaki C, Yanagi A, Yoshizane Y, Fujikawa K, Watashi K, Abe H, Wakita T, Hayes CN, Chayama K, et al.: Novel robust in vitro hepatitis B virus infection model using fresh human hepatocytes isolated from humanized mice. *Am J Pathol* 2015, 185:1275-1285.
56. Jurgens MC, Voros J, Rautureau GJP, Shepherd DA, Pye VE, Muldoon J, Johnson CM, Ashcroft AE, Freund SMV, Ferguson N: The hepatitis B virus preS1 domain hijacks host trafficking proteins by motif mimicry. *Nature Chemical Biology* 2013, 9:540-U532.
57. Ni Y, Lempp FA, Mehrle S, Nkongolo S, Kaufman C, Falth M, Stindt J, Koniger C, Nassal M, Kubitz R, et al.: Hepatitis B and D Viruses Exploit Sodium Taurocholate Co-transporting Polypeptide for Species-Specific Entry into Hepatocytes. *Gastroenterology* 2014, 146:1070-U1301.
58. Cai D, Nie H, Yan R, Guo JT, Block TM, Guo H: A southern blot assay for detection of hepatitis B virus covalently closed circular DNA from cell cultures. *Methods Mol Biol* 2013, 1030:151-161.
59. Wei CW, Ni CF, Song T, Liu Y, Yang XL, Zheng ZR, Jia YX, Yuan YA, Guan K, Xu Y, et al.: The Hepatitis B Virus X Protein Disrupts Innate Immunity by Downregulating Mitochondrial Antiviral Signaling Protein. *Journal of Immunology* 2010, 185:1158-1168.
60. Lu HL, Liao F: Melanoma differentiation-associated gene 5 senses hepatitis B virus and activates innate immune signaling to suppress virus replication. *J Immunol* 2013, 191:3264-3276.
61. Sato S, Li K, Kameyama T, Hayashi T, Ishida Y, Murakami S, Watanabe T, Iijima

S, Sakurai Y, Watashi K, et al.: The RNA Sensor RIG-I Dually Functions as an Innate Sensor and Direct Antiviral Factor for Hepatitis B Virus. *Immunity* 2015, 42:123-132.

62. Verrier ER, Wieland S, Baumert TF: RIG-I and Sensing of Hepatitis B Virus Revisited. *Hepatology* 2015, doi: 10.1002/hep.27935.
63. Roingeard P, Sureau C: Ultrastructural analysis of hepatitis B virus in HepG2-transfected cells with special emphasis on subviral filament morphogenesis. *Hepatology* 1998, 28:1128-1133.
64. Chou YC, Jeng KS, Chen ML, Liu HH, Liu TL, Chen YL, Liu YC, Hu CP, Chang C: Evaluation of transcriptional efficiency of hepatitis B virus covalently closed circular DNA by reverse transcription-PCR combined with the restriction enzyme digestion method. *J Virol* 2005, 79:1813-1823.
65. Liu ZQ, Mahmood T, Yang PC: Western blot: technique, theory and trouble shooting. *N Am J Med Sci* 2014, 6:160.
66. Nagashima K, Zheng J, Parmiter D, Patri AK: Biological tissue and cell culture specimen preparation for TEM nanoparticle characterization. *Methods Mol Biol* 2011, 697:83-91.
67. Noda T, Sagara H, Yen A, Takada A, Kida H, Cheng RH, Kawaoka Y: Architecture of ribonucleoprotein complexes in influenza A virus particles. *Nature* 2006, 439:490-492.

Acknowledgement

This thesis is based on material contained in the following scholarly paper.

[Name of author(s)]

Wan-Ling Yao, Sotaro Ikeda, Yuta Tsukamoto, Keiko Shindo, Yukie Otakaki, Main Qin, Yoshikazu Iwasawa, Fumihiko Takeuchi, Yuki Kaname, Yu-Chi Chou, Chungming Chang, Koichi Watashi, Takaji Wakita, Takeshi Noda, Hiroki Kato, and Takashi Fujita

[Title]

Establishment of a human hepatocellular cell line capable of maintaining long-term replication of hepatitis B virus

[Publication details] *International Immunology*, in press, 2017

I do appreciate Prof. Fujita and associate prof. Kato for their direction on this work. I have been working in this lab for more than three years, and I have learned many things related to study, life abroad, friendship, and social relationship. During these years, I made many good friends in this lab and outside the lab that have enriched my life in Japan. Mostly, I learned how to communicate with people from different cultures and countries. I appreciate all lab members for their aid, especially HBV team members. Our team is the first group to have short discussions for data sharing and new discoveries in other groups' publications. Sometimes, I made some mistakes and faced many difficulties, but I do thank prof. Fujita for his generous mind and useful suggestions to lead and direct me. Also with the kind help from prof. Kato, I always received suggestive words and comments from him. Sincerely, I am so grateful to say I appreciate all the friendly assistance from lovely people here. Last, I would also like to mention this work was supported by the grant from AMED, MEXT, and JSPS. Thank you for all the help from **Fujita's lab** and the **Graduate School of Biostudies.**